



# MRI and In Vivo Spectroscopy of the Brain

# 8

Matthew T. Whitehead and Andrea Gropman

## Contents

<b>Introduction</b> .....	96
<b>Intoxication Type Disorders/Acute Metabolic Encephalopathy</b> .....	97
<b>Maple Syrup Urine Disease (MSUD)</b> .....	97
<b>Nonketotic Hyperglycinemia (NKH)</b> .....	99
<b>Methylmalonic Aciduria (MMA)</b> .....	100
<b>Glutaric Aciduria Type I</b> .....	100
<b>L-2-Hydroxyglutaric Aciduria</b> .....	100
<b>Urea Cycle Disorders (UCD)</b> .....	100
<b>Molybdenum Cofactor Deficiency</b> .....	102
<b>Chronic Metabolic Encephalopathies</b> .....	102
<b>Phenylketonuria (PKU)</b> .....	102
<b>Pantothenate Kinase-Associated Neurodegeneration (PKAN)</b> .....	103
<b>Menkes Disease</b> .....	104
<b>Congenital Disorders of Glycosylation (CDG)</b> .....	104
<b>Neuronal Ceroid Lipofuscinosis (NCL)</b> .....	105
<b>Mucopolysaccharidoses (MPS)</b> .....	105
<b>Mitochondrial Disorders</b> .....	106
<b>Leigh Disease</b> .....	106
<b>MELAS Syndrome</b> .....	106
<b>White Matter Disorders/Leukodystrophies</b> .....	108
<b>X-linked Adrenoleukodystrophy (X-ALD)</b> .....	108
<b>Zellweger Syndrome</b> .....	108
<b>Aicardi-Goutieres Syndrome (AGS)</b> .....	109
<b>Krabbe Disease</b> .....	109

M. T. Whitehead (✉)  
Department of Radiology, Children's National Health System,  
Washington, DC, USA  
e-mail: [MWhitehe@childrensnational.org](mailto:MWhitehe@childrensnational.org)

A. Gropman  
Department of Neurology, Children's National Health System,  
Washington, DC, USA  
e-mail: [agropman@childrensnational.org](mailto:agropman@childrensnational.org)

<b>Metachromatic Leukodystrophy (MLD)</b> .....	109
<b>Canavan Disease</b> .....	111
<b>tRNA Synthetase Disorders</b> .....	111
<b>Substrate Depletion Disorders</b> .....	111
<b>Creatine Deficiency Syndromes</b> .....	111
<b>References</b> .....	144

## Summary

Most inborn errors of metabolism (IEMs) have a potential for central nervous system (CNS) injury resulting in chronic encephalopathy. IEMs may affect CNS structures in a manner dependent upon disorder type, stage of brain development, severity, and/or duration. Several of the disorders share a final common pathway to brain dysfunction such as disruption of astrocyte function, excitotoxicity, and/or energy failure.

Neuroimaging has emerged as a powerful clinical tool to study the brain in a noninvasive manner in order to assist in distinguishing disorders from one another, despite very similar clinical manifestations. As there are limited ways in which the CNS can respond to insults, imaging manifestations are often nonspecific. Nonetheless, there is a striking anatomical pattern of vulnerability in many IEMs. Some IEMs cause reasonably predictable disease patterns that can be suggestive or diagnostic. Specific neuroimaging patterns of inborn metabolic errors are the focus of this chapter.

## Introduction

It is important to alert the radiologist or neuroradiologist whenever there is clinical concern for a metabolic abnormality affecting the CNS. The MRI armamentarium contains numerous sequences that can be chosen to identify alterations in brain structure, texture, water movement, metabolism, and mineralization and to detect hemorrhage. Time constraints limit sequence selection to only those most necessary and relevant. Therefore, the provided history should be as specific as possible to ensure that the imaging exam will be tailored using an appropriate pulse-sequence prescription most likely to determine the IEM type and/or answer the clinical question. “New onset generalized seizures and developmental regression” is an example of an adequate history, while “encephalopathy” is more nonspecific and “rule out pathology” is simply unacceptable. “Rule out x” is never appropriate in isolation, but welcomed after explaining *why* x needs to be excluded. Pertinent lab values and head circumference are useful to include in the neuroim-

aging order request in some cases. A history of prematurely and estimated gestational age should always be disclosed as the expected normal appearance of the brain changes over time, especially with regard to myelination. This concept is best captured by the idiom “garbage in, garbage out.” Inadequate exam indications have a higher chance of yielding the unsavory phrase, “correlate clinically.”

Dominant factors influencing modality selection and examination protocols include patient age, past medical history (especially contraindications to contrast material and/or MRI), signs, symptoms, and the history of present illness. Head ultrasound is often the initial imaging exam in the neonatal setting given its near universal access, portability, ease of acquisition, and lack of ionizing radiation. Drawbacks of ultrasound include a relative insensitivity and poor specificity for brain pathology. CT excels in the detection of calcifications and hemorrhage. It can also be useful in the acute setting to quickly identify actionable intracranial abnormalities and when sonographic findings require clarification. However, MRI is the reigning gold standard in the neuroimaging assessment of the CNS. In addition to its ability to demonstrate multiplanar fine structural details, it exploits inherent and acquired differences in tissue properties to reveal changes in disease states. Therefore, the sensitivity and specificity of MRI generally exceed those of ultrasound and CT.

A typical brain MR protocol for suspected metabolic abnormalities should include both conventional sequences (i.e., T1WI, T2WI) and advanced imaging techniques such as diffusion tensor imaging, perfusion, and proton magnetic resonance spectroscopy (1H MRS). A magnetization transfer sequence is also useful in the evaluation of leukodystrophies to determine the type of white matter disturbance. Intravenous gadolinium-based contrast agents (GBCAs) may be useful when the specific diagnosis is uncertain as these add specificity to some IEMs and help exclude mimics such as infection and subacute infarction. Spine MR imaging can also be useful in some disorders to improve diagnostic specificity.

1H MRS has great utility in the initial work-up and subsequent follow-up of metabolic disturbances/disorders. Although a nonspecific pattern (elevated choline, depressed NAA) is common in many types of brain disease, short echo 1H MRS (TE < 40 ms) can reveal more specific metabolic signatures. Furthermore, temporal changes on subsequent exams can support or refute the benefit of ongoing

therapeutic measures. A simple single voxel technique boasts better signal-to-noise ratios and allows shorter TE options when compared with multivoxel technique (Bluml and Panigrahy 2013). Voxel size is a balance between signal-to-noise (SNR) and tissue specificity; ideally, it should be as large as possible to achieve satisfactory SNR but small enough to target the area of interest. Generally, a  $2 \times 2 \times 2$  cm voxel is used; voxels smaller than  $1 \text{ cm}^3$  are unlikely to be worthy of the acquisition time it would require to achieve reasonable SNR. Voxel location and echo times should be selected based on the suspected and/or discovered disease patterns. Hemorrhage, iron, and calcification hamper  $^1\text{H}$  MRS quality and impact SNR; these should be avoided, and if unavoidable,  $^1\text{H}$  MRS should not be performed as misleading information could be returned. In our experience, two acquisitions using two different echo (short and longer) are more useful and preferable to one whenever feasible. The reasons are multifactorial, but some notable issues relate to the fact that metabolites in small concentrations tend to be more visible using short echo times, metabolic peak overlap may be more or less apparent at different echo times, J coupling and J modulation are altered at different echo times, longer echo times have less inherent noise, and metabolites have different T2 properties. We typically perform ultrashort (TE 14, TR 1500; STEAM technique), short (TE 35, TR 1500–2000; PRESS technique), and intermediate (TE 144, TR 1500–2000; PRESS) or long (TE 288, TR 1500–2000; PRESS) echo time sequences. Magnetic field strength dictates the choice of the longest echo time; because lactate detection is unreliable at 144 ms TE at 3 T field strength, we use a 288 ms TE at 3 T instead (Lange et al. 2006).

The vast majority of inborn errors of metabolism (IEM) have a nonspecific neuroimaging phenotype. Imaging manifestations often overlap among IEMs and more broadly with other CNS diseases. This is especially true at the extremes of the disease time course where normal exams may be found early on and in presymptomatic individuals, and diffuse chronic brain changes are often present in the end-stage patient. However, some IEMs tend to be more specific, and others can be diagnostic using MRI and/or MRS. After a deviation from the age-expected normal appearance is recognized, the next step in interpretation is to determine the disease pattern, if present, using images from all available modalities and time points. Several imaging features raise concern for the possibility of an IEM: symmetric abnormalities in brain signal/density/echogenicity, disease patterns atypical for ischemic and infectious insults, mixed aged lesions, temporal variability inconsistent with the expected evolution of a static encephalopathy, and unexpected spectroscopic abnormalities. Of course, the imaging results should always be interpreted in the context of the clinical picture. Metabolic disorders with suggestive or diagnostic neuroimaging appearances in the therapeutic naive state are discussed in the following paragraphs with associated figures.

## Intoxication Type Disorders/Acute Metabolic Encephalopathy

**The disorders typically defined as intoxication type share a similar clinical presentation. Several groups of IEM including the organic acidemias, urea cycle disorders, and certain disorders of amino acid metabolism typically present with acute life-threatening symptoms and a rapidly evolving encephalopathy. These symptoms are the result of a toxic accumulation of metabolites in the CNS. Symptoms may include seizures, apnea, respiratory distress, and lethargy progressing to coma due in part to ensuing brain edema. While nonspecific in nature and clinically difficult to differentiate the underlying diagnosis, several of these diseases have characteristic imaging patterns, some of which are illustrated below.**

### Maple Syrup Urine Disease (MSUD)

Neonatal encephalopathy is the most common presentation of this aminoacidopathy. Marked, extensive brain edema is typical, comprised of mixed subtypes: vasogenic edema in unmyelinated white matter and intramyelinic edema in myelinating white matter (Whitehead and Gropman 2018; Jan et al. 2003; Sakai et al. 2005; Terek et al. 2013; Ha et al. 2004). White matter reduced diffusion is usually quite profound, especially in the projectional fibers, thalami, globus pallidus, pontocerebellar fibers, and deep cerebellar nuclei (Whitehead and Gropman 2018; Jan et al. 2003; Ha et al. 2004; Barkovich and Patay 2019) (Fig. 8.1). Diffusion abnormalities may in part reflect spongiotic dysmyelination with intramyelinic edema rather than demyelination given the lack of magnetization transfer signal, prolonged persistence in patients under dietary control, and the presence in presymptomatic patients (Terek et al. 2013; Ha et al. 2004; Sener 2002; Myers et al. 2012). Diffusion abnormalities in more maturely myelinated brains may be more widespread (Sakai et al. 2005). Milder phenotypes may show only hypomyelination and mild atrophy, T2 prolongation in the globus pallidus, and/or deep cerebral white matter hyperintensity (Ishikawa et al. 1991; Li et al. 1997; Muller et al. 1993). In adolescent and adults, extensive cerebral cortical restricted can occur during metabolic decompensation (Jan et al. 2003). Central spinal cord T2 prolongation has been shown in a sibling pair with MSUD (Bhat et al. 2013).

MRS shows multiple enlarged macromolecular peaks corresponding to branched chain amino acids (BCAAs), branched chain ketoacids (BCKAs), lipid, and lactate along with elevated choline and myoinositol and depressed *N*-acetylaspartate (NAA) (Bluml and Panigrahy 2013; Jan et al. 2003; Terek et al. 2013) (Fig. 8.1). Notably, longer echo times improve diagnostic specificity in MSUD by eliminating the normal background macromolecular signal that can hide BCAA/BCKA peaks (Jan et al. 2003).

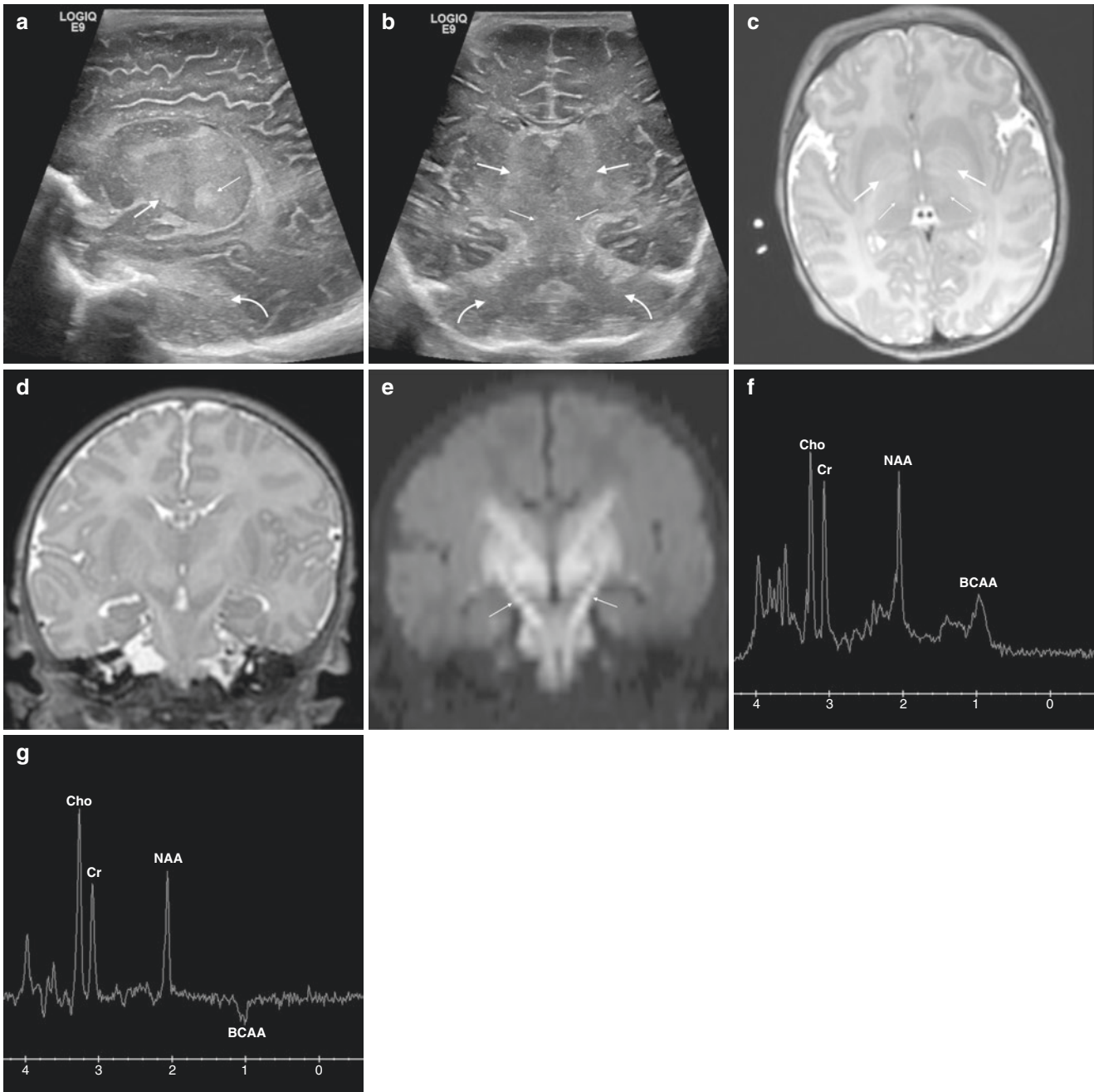


**Fig. 8.1** Neonatal female with maple syrup urine disease (MSUD). (a) Parasagittal gray-scale ultrasound image of the brain shows abnormal hyperechogenicity in the cerebral white matter, lentiform nuclei (thick arrow), thalamus (thin arrow), and imaged cerebellum representing edema (curved arrow). (b) Coronal gray-scale ultrasound image of the brain shows thalamic (thick arrows), brainstem (thin arrow), and cerebellar (curved arrow) hyperechogenicity representing edema. (c) Axial T2-weighted MR image (TR/TE msec, 2500/65) through the basal ganglia depicts abnormal hyperintense signal in parts of the globi pallidi (thick arrows), thalami (thin arrows), and white matter. Coronal T2WI

(TR/TE msec, 2500/65) (d) and corresponding diffusion weighted image (TR/TE msec, 8000/84) (e) in a similar plane to (b) show signal abnormality and reduced diffusion representing intramyelinic edema in the basal ganglia, thalamus, and brainstem with notable involvement of projectional fibers representing intramyelinic edema (arrows, e). Single voxel MRS over the left basal ganglia (TR/TE msec, 1500/35) (f) and (TR/TE msec, 1500/144) (g) reveal a broadened metabolic peak at 0.9–1.1 ppm that inverts on the longer echo time MRS (arrows), representing branch chain amino acids/branch chain keto acids (BCAA)



## Nonketotic Hyperglycinemia (NKH)

NKH is an amino acidopathy that typically presents in the neonatal period with encephalopathy, seizures, and hypotonia. Neuroimaging features can be quite specific when MRI and <sup>1</sup>H MRS are obtained and interpreted in parallel. Namely, intramyelinic edema manifested by reduced diffusion can be seen in the myelinating fibers of the cerebrum, cerebellum, and brainstem, with excessive hyperintense signal on T2WI in the unmyelinated white matter either representing undermyelination and/or vasogenic edema (Whitehead and Gropman 2018; Whitehead et al. 2015; Stence et al. 2019) (Fig. 8.2). These changes occur in similar locations as those found in maple syrup urine disease (MSUD), but are typically much less severe and

extensive. The corpus callosum is often hypogenetic and the total brain volume small (Whitehead and Gropman 2018; Whitehead et al. 2015; Stence et al. 2019) (Fig. 8.2). Wei and colleagues reported a case of long tract hyperintensity on T2WI spanning from the dorsal medulla into the cervical and thoracic dorsomedial spinal cord (Wei et al. 2011).

<sup>1</sup>H MRS reveals elevated glycine at 3.55 ppm that correlates more reliably with the clinical status than plasma and CSF glycine concentrations (Bluml and Panigrahy 2013; Whitehead and Gropman 2018; Whitehead et al. 2015; Heindel et al. 1993) (Fig. 8.2). It is necessary to obtain at least one <sup>1</sup>H MRS data point using an intermediate (i.e., 144 ms) or long (i.e., 288 ms) echo time to remove the spectral contamination of MI around 3.5 ppm.

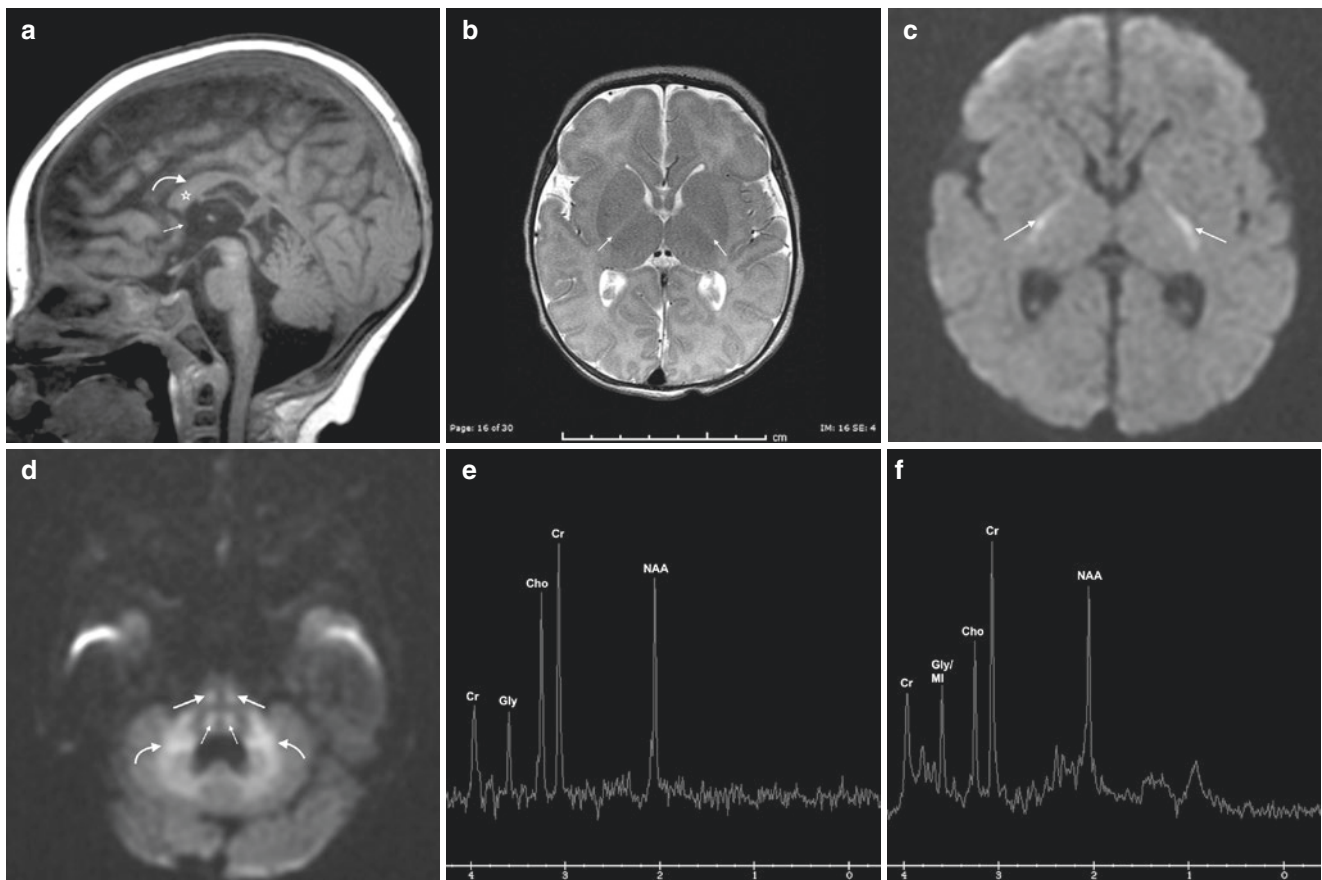


**Fig. 8.2** Neonatal female with nonketotic hyperglycinemia. (a) Sagittal midline T1WI (TR/TE msec, 7/2) demonstrates multiple structural midline abnormalities including a thin, shortened hypogenetic corpus callosum (curved arrow), marked hypoplasia of the anterior commissure (thin arrow), hypoplasia of the septum pellucidum (star), and mild pontine hypoplasia. (b) Axial T2WI (TR/TE msec, 3183/96) at the level of the basal ganglia shows lack of normal myelination-related hypointensity of the posterior limb of the internal capsule (PLIC) (arrows). Axial DWI (TR/TE msec, 80,000/85) through the

basal ganglia (c) and posterior fossa (d) shows increased signal/reduced diffusion in the PLIC (arrows, c), corticospinal tracts (thick arrows, d), central tegmental tracts (thin arrows, d), and middle cerebellar peduncles/deep cerebellar white matter (curved arrows, d). Single voxel MRS over the left basal ganglia (TR/TE msec, 1500/144) (e) and (TR/TE msec, 1500/35) (f) reveals an abnormal metabolic peak at 3.6 ppm that overlaps with myoinositol on the short echo MRS consistent with glycine (gly). Creatine (Cr) is elevated, while choline (Cho) is mildly depressed, altering the normal ratios of NAA, Cr, and Cho

## Methylmalonic Aciduria (MMA)

Typical presentation of metabolic acidosis and coma is not enough to differentiate this clinically from other intoxication disorders. In MMA, the basal ganglia are commonly affected with or without concurrent involvement of the substantia nigra and dentate nuclei. In particular, the globus pallidi are involved dominantly or in isolation (Whitehead and Gropman 2018). In decompensation, reduced diffusion is present in the basal ganglia, and chronic injury leads to regional volume loss and hyperintense signal on T2WI with facilitated diffusion (Fig. 8.3). Lactic acidosis is often shown on 1H MRS (Bluml and Panigrahy 2013).

## Glutaric Aciduria Type I

This IEM may be differentiated clinically due to movement disorders that may present acutely and may have associated macrocrania. On MRI, hyperintense basal ganglia signal on T2WI with restricted diffusion sparing the thalami may be found in acute symptomatic patients (Whitehead and Gropman 2018; Barkovich and Patay 2019; Whitehead et al. 2015) (Fig. 8.4). Cerebral white matter hyperintensity and cerebellar deep gray nuclear involvement may also be present. Important structural features that help distinguish glutaric aciduria from other IEMs include underopercularization and enlarged extra-axial spaces in the middle cranial fossae (Whitehead and Gropman 2018; Barkovich and Patay 2019; Whitehead et al. 2015) (Fig. 8.4). Progressive atrophy often leads to development of nontraumatic subdural hemorrhage. Glutaric acid has been found using 1H MRS, along with reduced NAA and creatine, elevated choline, and lactate (Bluml and Panigrahy 2013; Harting et al. 2015).

## L-2-Hydroxyglutaric Aciduria

In this rare IEM, clinical symptoms overlap with those of other intoxicating disorders. Conversely, neuroimaging features are quite suggestive when present, as this is one of the few disorders that manifests a centropedal cerebral lesion severity gradient from superficial to central (Barkovich and Patay 2019; Fourati et al. 2016) (Fig. 8.5). Thus, subcortical precedes deep white matter involvement, and external and extreme capsules are affected prior to the deep gray structures. Cerebellar deep gray nuclei are also quite commonly affected (Barkovich and Patay 2019; Fourati et al. 2016). In addition to decreased NAA and choline concentrations, L-2-hydroxyglutaric acid elevation has been suggested on MRS at 2.5 ppm (Fourati et al. 2016; Anghileri et al. 2016).

## Urea Cycle Disorders (UCD)

Acute metabolic decompensation associated with hyperammonemia (HA) and intermediate metabolite toxicity causes brain swelling, edema, and variable injury, especially in the neonatal period and more commonly in complete proximal urea cycle defects (Helman et al. 2014; Pacheco-Colon et al. 2013). Patients may have mild (partial deficiencies, later onset) to severe HA (infant onset). There is a metabolic alkalosis that can, for example, help distinguish UCD from MMA that can have lower levels of HA. Disease patterns may vary based on the specific enzymatic or transporter defect, though phenotypic similarities are common among UCD subtypes (Barkovich and Patay 2019). The most familiar imaging patterns are “diffuse” and “central” with the latter isolated to the insular/peri-insular, perisylvian, perirolandic, internal capsular, and/or basal ganglia regions

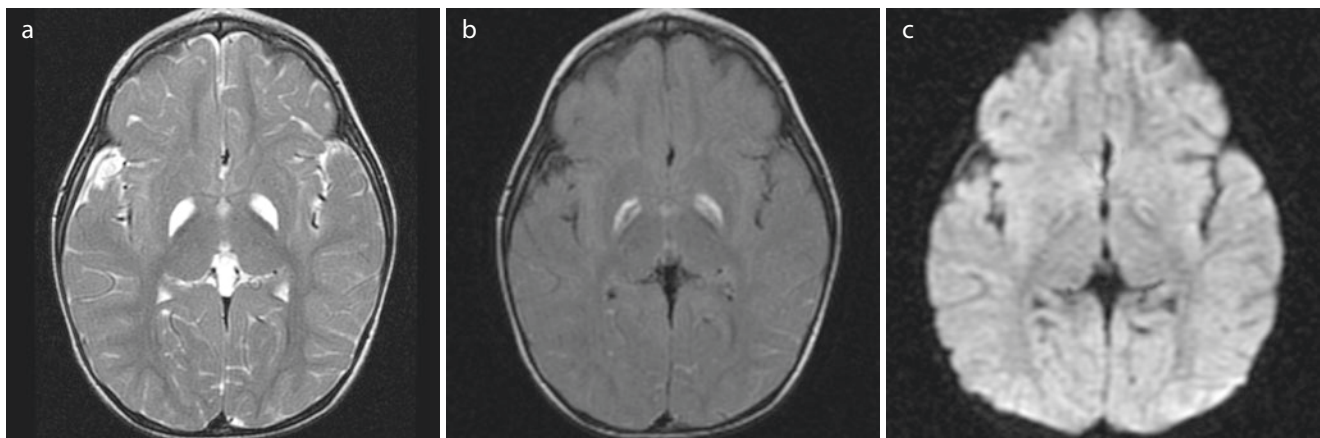


**Fig. 8.3** A 15-year-old female with methylmalonic aciduria. (a) Axial T2WI (TR/TE msec, 4217/101) through the basal ganglia shows hyperintense globi pallidi. The corresponding T2/FLAIR sequence (TR/TE/ TI msec, 10,000/136/2200) (b) and diffusion-weighted sequence (TR/

TE msec, 9300/93) (c) demonstrate mixed globi pallidi signal changes with central suppression/necrosis and peripherally reduced diffusion, representing acute on chronic metabolic injury

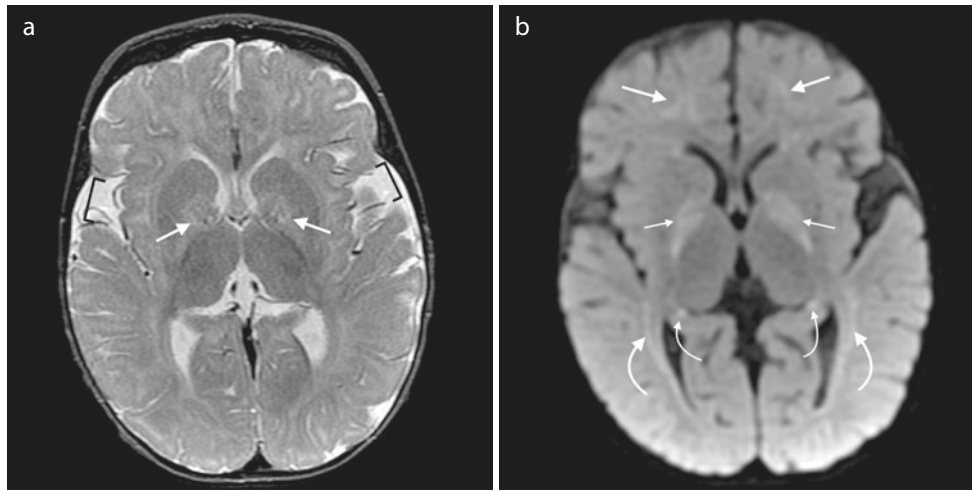


**Fig. 8.4** A 9-month-old female with glutaric aciduria type I. (a) Axial T2WI (TR/TE msec, 3200/90) through the basal ganglia reveals hyperintense signal in the globi pallidi (arrows) and underopercularization (brackets). (b) The corresponding axial diffusion-weighted image (TR/TE msec, 10,000/91) shows hyperintense signal in the globi pallidi

(small straight arrows), frontal subcortical white matter (large straight arrows), sagittal stratum (large curved arrows), and hippocampal tails (small curved arrows) representing reduced diffusion/white matter intramyelinic edema and seizure-related changes in the hippocampi

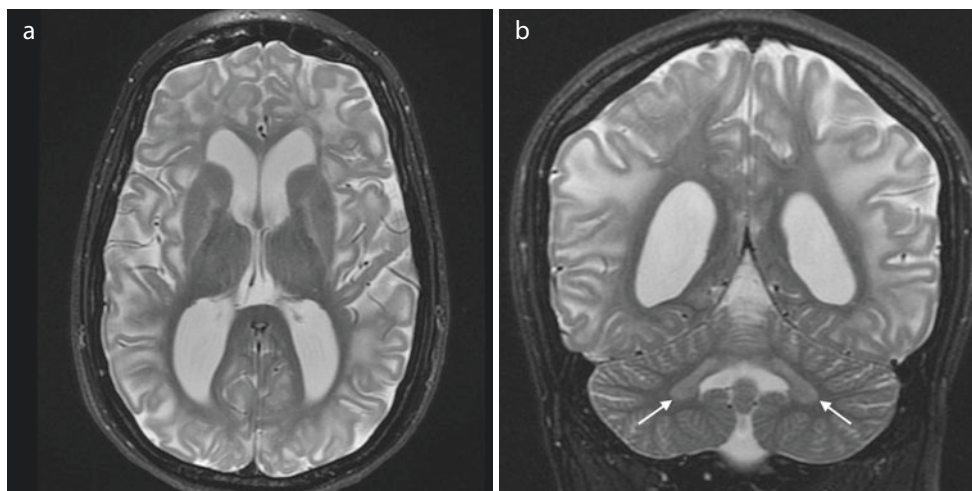


**Fig. 8.5** A 2-year-old female with L-2-hydroxyglutaric aciduria. (a) Axial T2WI (TR/TE msec, 5347/101) at level of the basal ganglia shows a centropedal pattern of white matter hyperintensity affecting the superficial more than deep white matter with relative sparing of the cor-

pus callosum. (b) Coronal T2WI (TR/TE msec, 5347/101) redemonstrates the centropedal pattern of white matter hyperintensity and shows abnormal hyperintensity of the cerebral deep gray nuclei (arrows). Ventriculomegaly reflects white matter volume loss

(Barkovich and Patay 2019; Gunz et al. 2013; Takanashi et al. 2003; Bireley et al. 2012) (Fig. 8.6). An unsolicited imaging diagnosis can be tricky as UCD disease patterns overlap considerably with that of the far more common hypoxic ischemic encephalopathy (HIE) (Whitehead and Gropman 2018; Pacheco-Colon et al. 2013).

UCD brain edema is often mixed; vasogenic (facilitated diffusion), cytotoxic (gray matter, restricted diffusion), and/or intramyelinic (white matter, restricted diffusion) edema may be present depending on the imaging timing and disease activity. Diffusion abnormalities evolve quickly toward

hyperintense signal on T1WI, representing laminar, deep gray, and white matter necrosis with associated volume loss. In all but the most severe cases, the thalami and brainstem are spared, which may help distinguish it from HIE (Whitehead and Gropman 2018; Barkovich and Patay 2019; Pacheco-Colon et al. 2013; Bireley et al. 2012). Also, a perinsular and cingulate predilection can be a clue, but these structures may also be involved in HIE as well (Whitehead and Gropman 2018; Barkovich and Patay 2019). In distal UCD subtypes, later onset cases, and/or milder phenotypes, brain lesions and volume deficits tend to be less severe and



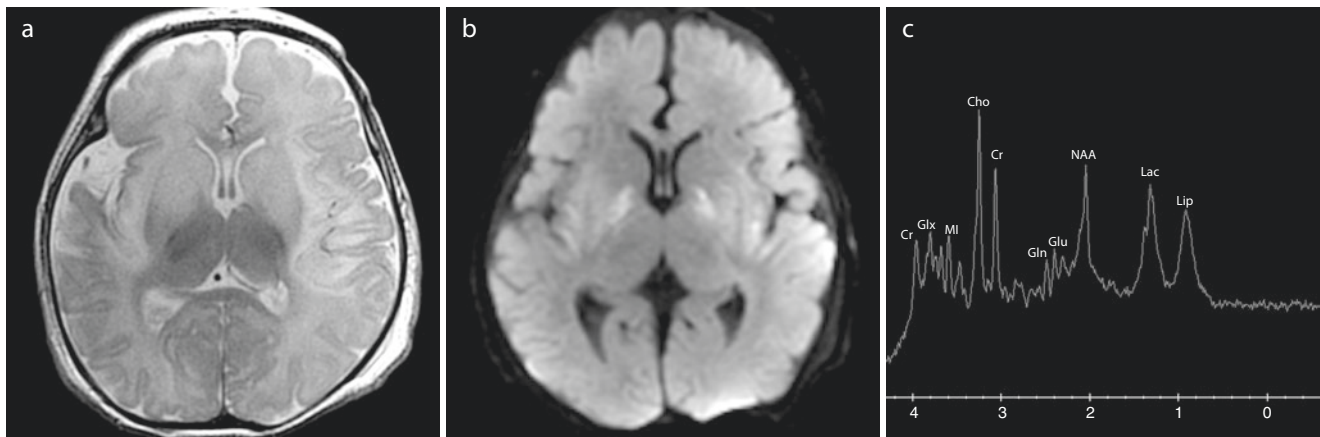


**Fig. 8.6** A 10-day-old male with citrullinemia (argininosuccinate synthetase deficiency). (a) Axial T2WI (TR/TE msec, 5725/78) at the level of the basal ganglia shows cortical/subcortical temporo-insular/perisylvian predominant and striatal hyperintensity consistent with edema; note thalamic sparing. The corresponding DWI (TR/TE msec, 10,000/95) (b) shows reduced diffusion in the same regions represent-

ing cytotoxic and intramyelinic edema. Short echo single voxel MRS over the left basal ganglia (TR/TE msec, 1500/35) (c) shows elevated glutamine (Gln), glutamate (Glu), lipids (Lip), and lactate (Lac) with reduced myoinositol (MI). Elevated alpha proton-associated metabolic peak at 1.8 ppm confirms glutamine and glutamate elevation (Glx)

less extensive. In these cases, DTI can reveal decreased microstructural integrity in otherwise normal appearing white matter (Pacheco-Colon et al. 2013; Gropman et al. 2008a, b).

1H MRS can reveal elevated brain glutamine and glutamate in presymptomatic, symptomatic, convalescent, and asymptomatic phases (Pacheco-Colon et al. 2013; Gropman et al. 2008a, b) (Fig. 8.6). Myoinositol, an osmotic buffer, is typically depressed prior to and is inversely correlated with glutamine concentration (Pacheco-Colon et al. 2013; Gropman et al. 2008a, b). Accumulated guanidinoacetate has been shown in arginosuccinate lyase deficiency (Sijens et al. 2006). Arginine elevation has been described in arginase deficiency (Gungor et al. 2008).

## Molybdenum Cofactor Deficiency

A devastating neonatal IEM, molybdenum cofactor deficiency results in massive destructive changes throughout the cerebral white matter and deep gray structures with progression to cystic necrosis and marked volume loss (Whitehead and Gropman 2018; Barkovich and Patay 2019; Schuierer et al. 1995; Stence et al. 2013) (Fig. 8.7). Lesional hemorrhages and deep gray nuclear and/or cerebral white matter calcifications may also be present. Widespread cortical restricted diffusion has also been described, especially affecting sulcal depths and leading to ulegyria (Stence et al. 2013). Changes can mimic HIE, but the pattern is less typical, often sparing the thalami, and destruction more severe in the majority of cases. Mixed aged lesions, pontocerebellar hypoplasia, and enlarged cisterna magna are additional fea-

tures that favor molybdenum cofactor deficiency over HIE. Disease onset can be either pre- or postnatal; cystic necrosis encountered in the first week of life is most indicative of a prenatal onset. MRS may show elevated lipid and lactate in the active phase of disease (Salvan et al. 1999).

## Chronic Metabolic Encephalopathies

**Several of the IEMs do not typically present initially with an acute decompensation, but rather with ongoing brain injury in recognizable patterns. These are discussed below.**

### Phenylketonuria (PKU)

Phenylketonuria, an autosomal recessive condition, is characterized by deficiency in phenylalanine hydroxylase, an essential precursor to an array of neurotransmitters, notably dopamine which is critically involved in higher order cognition. The majority of patients have extensive white matter damage, in both untreated and early treated PKU cases. Classic MR imaging features include posterior predominant cerebral periventricular hyperintensity on T2WI with or without reduced diffusion, usually sparing the juxtacortical white matter, cortex, brainstem, and cerebellum (Whitehead and Gropman 2018; Anderson and Leuzzi 2010; Kono et al. 2005) (Fig. 8.8). White matter diffusion restriction reflecting intramyelinic edema tends to occur when plasma phenylalanine levels exceed 8.5 mg/dL (Kono et al. 2005).



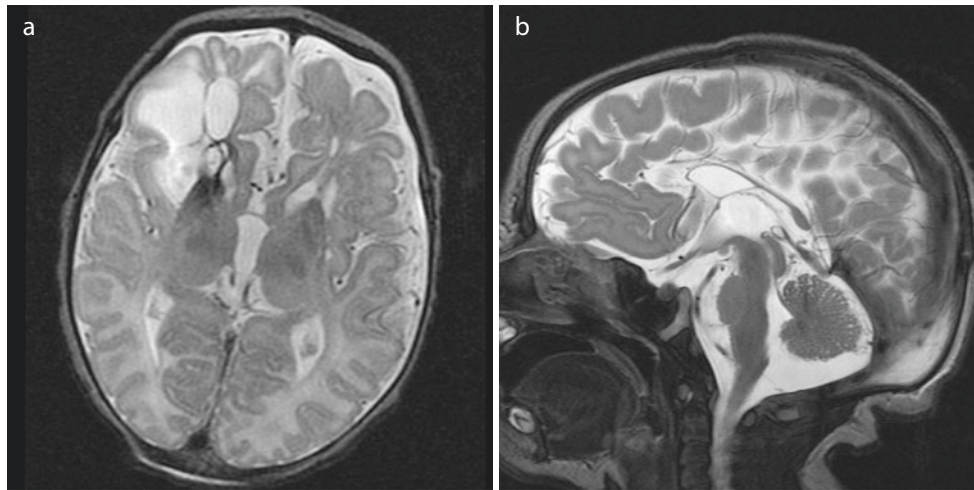


**Fig. 8.7** A 3-day-old female with molybdenum cofactor deficiency. (a) Axial T2WI (TR/TE msec, 3500/126) at the level of the basal ganglia demonstrates frontal volume loss and heterogenous, mixed hyperintense and hypointense signal in the basal ganglia and frontal white matter, right more than left, consistent with chronic sequela of prior

hemorrhages and infarctions with resultant cystic/necrotic encephalomalacia. (b) Sagittal midline T2WI (TR/TE msec, 3500/126) shows marked thinning of the corpus callosum most pronounced anteriorly reflecting the cerebral white matter volume loss

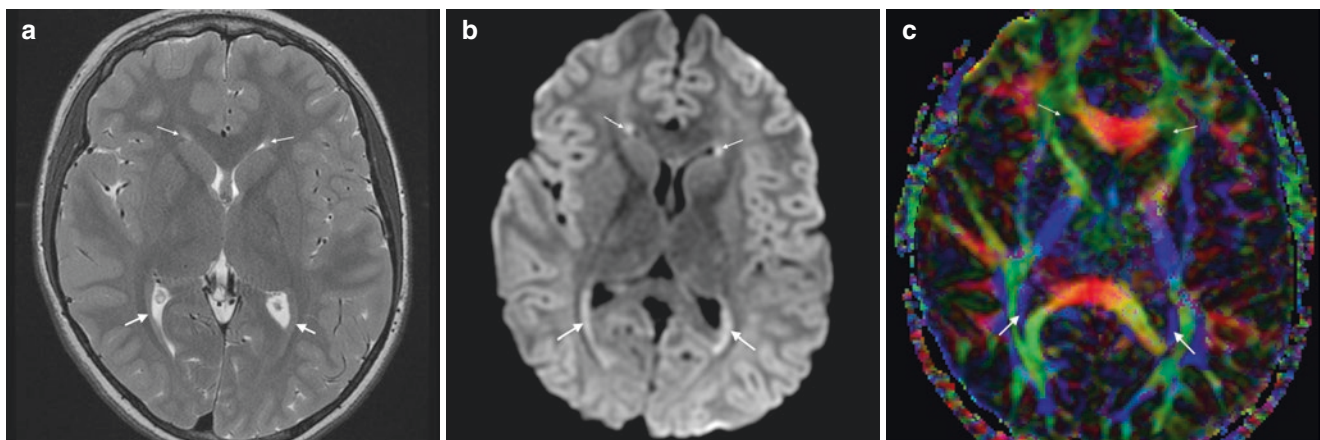


**Fig. 8.8** A 9-year-old male with phenylketonuria (PKU). Axial T2WI (TR/TE msec, 3350/102) (a) and corresponding DWI (TR/TE msec, 10,000/82) (b) at the level of the basal ganglia show hyperintense signal in the paraventricular frontal and temporo-occipital tissues; in correla-

tion with the directionally encoded DTI color map (c), the signal changes correspond to myelin edema in the frontal subependymal white matter fibers (small arrows) and temporo-occipital tapetum (large arrows), typical sites of PKU-associated intramyelinic edema

<sup>1</sup>H MRS in isolation or in combination with MRI is specific to the diagnosis when correctly performed using a specialized short-echo sequence and postprocessing to identify the generally small phenylalanine peak at 7.3–7.4 ppm downstream beyond the suppressed water peak (Bluml and Panigrahy 2013). The alpha proton associated with elevated phenylalanine can be seen at 3.8 ppm; however, there is considerable overlap with other metabolites at this same location (Sener 2003). NAA, creatine, choline, and other conventional metabolites tend to be normal.

### Pantothenate Kinase-Associated Neurodegeneration (PKAN)

A form of neurodegeneration with brain iron accumulation (NBAI), PKAN is classically known for its “eye of the tiger sign” on MRI (Fig. 8.9). Dark iron deposition in the globus pallidus and bright central necrosis contribute to this appearance. Accelerated iron deposition is also common in the substantia nigra, while the dentate nucleus is rarely affected (Hayflick et al. 2018). These features help distinguish PKAN

**Fig. 8.9** A 5-year-old male with pantothenate kinase-associated neurodegeneration (PKAN). Axial T2WI (TR/TE msec, 6350/97) (a) through the basal ganglia shows globi pallidi signal abnormality with peripheral hypointensity and central hyperintensity representing accelerated iron deposition and central necrosis, the “eye of the tiger” sign of PKAN (arrows). The corresponding axial gradient echo sequence (b) confirms increased iron deposits with dark susceptibility effect (arrows)

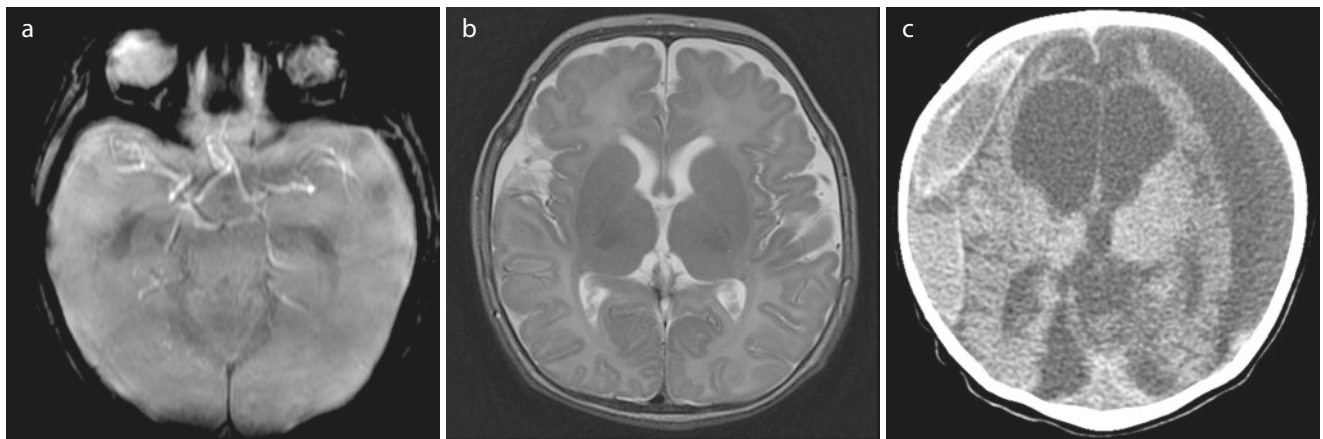
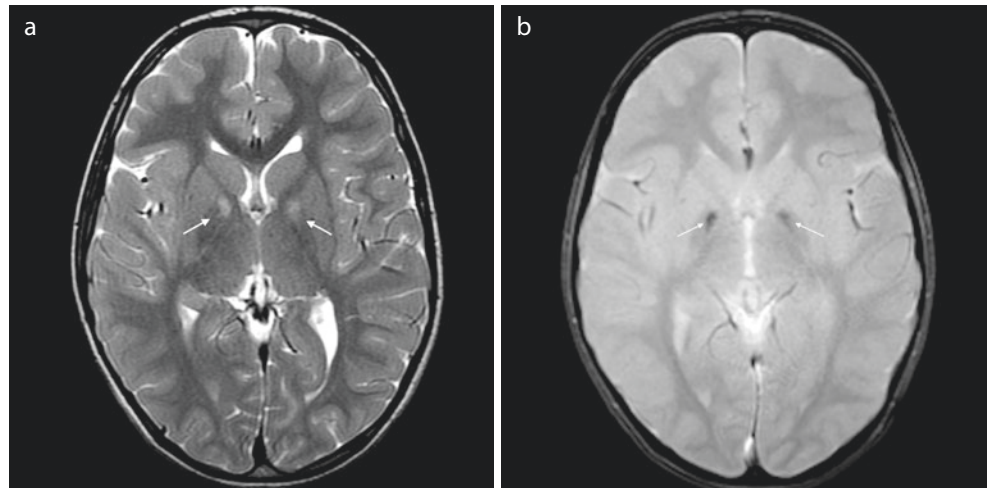


**Fig. 8.10** Menkes disease in a male child performed at 3 months (a, b) and 12 years (c) of age. (a) Axial susceptibility weighted angiography (SWAN; TR/TE msec, 68/24) at the level of the circle of Willis shows multiple tortuous, elongated intracranial arteries. (b) Axial T2WI (TR/

TE msec, 5900/91) of the cerebrum at the level of the basal ganglia is normal for age. (c) Follow-up head CT at age 12 years reveals interval development of bilateral subdural hemorrhages of varying age, marked parenchymal atrophy, and bilateral cerebral encephalomalacia

from other forms of NBAI, such as infantile neuroaxonal dystrophy that lacks “eye of the tiger sign,” beta-propeller protein-associated neurodegeneration (BPAN) with dominant substantia nigra involvement showing a hyperintense “halo”, and neuroferritinopathy and aceruloplasminemia where iron deposition is more widespread to name a few (Hayflick et al. 2018).

## Menkes Disease

Deficient tissue copper results in various vascular and brain abnormalities. Elongated, tortuous intracranial arteries have a disorganized, spaghetti-like appearance (Whitehead et al. 2015; Manara et al. 2017a, b) (Fig. 8.10). Cerebral white matter disease with delayed myelination and basal ganglia lesions are characteristic (Manara et al. 2017a, b). Transient

tumefactive temporal lobe vasogenic edema is reasonably common in the infantile period (Whitehead et al. 2015). Progressive volume loss and subdural hemorrhages are frequent features in the chronic disease stage (Manara et al. 2017a, b) (Fig. 8.10). MRS reveals lactate, reduced NAA, and/or increased choline in some cases (Ito et al. 2011; Munakata et al. 2005).

## Congenital Disorders of Glycosylation (CDG)

Reduced brain volume and variable signal changes are common in CDG. There are now over 30 subtypes of CDG. The prototypical subtype, CDG Type Ia, commonly shows pontocerebellar hypoplasia and superimposed cerebellar volume loss with cortical hyperintensity, referred to as the “shrunken, bright cerebellar sign” (Whitehead et al.



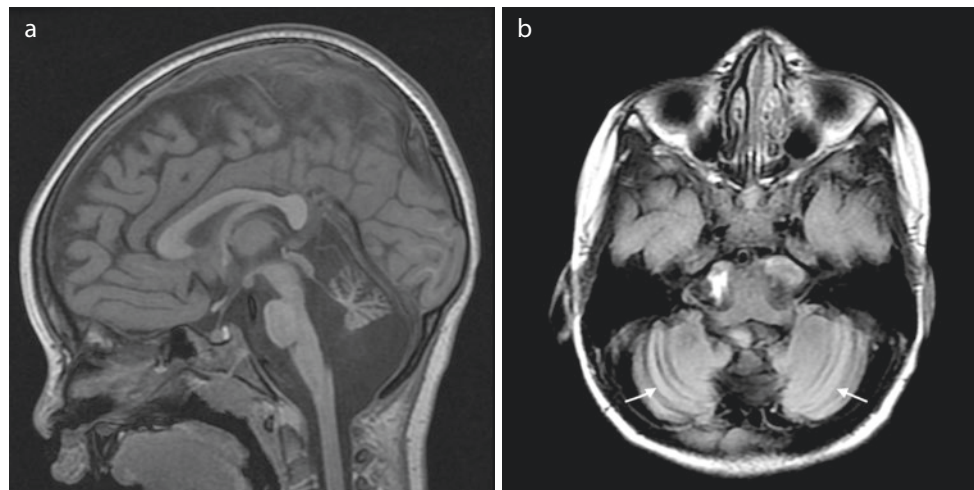
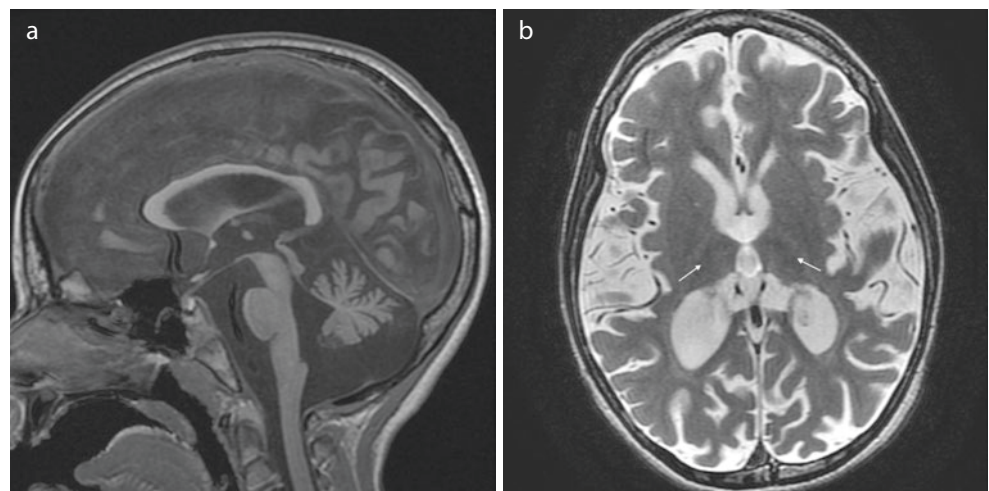


**Fig. 8.11** A 3-year-old male with congenital disorder of glycosylation type Ia. (a) Sagittal midline T1WI (TR/TE msec, 11/5) shows a markedly small cerebellum that is shortened with widened fissures representing combined volume loss and hypoplasia. Mild pontine hypoplasia is also present. The fourth ventricle and posterior fossa cisterna spaces

are enlarged secondary to the rhombencephalic volume deficit. (b) Axial T2 FLAIR image (TR/TE/TI msec, 10,000/126/2250) through the cerebellum shows volume loss and cortical hyperintensity, the “shrunken, bright cerebellar sign” consistent with CDG1a (arrows)

**Fig. 8.12** A 5-year-old female with neuronal ceroid lipofuscinosis. (a) Sagittal midline T1WI (TR/TE msec, 11/5) demonstrates diffuse moderate cerebral and cerebellar cortical volume loss with enlarged sulci, cerebellar fissures, and cisternal spaces. (b) Axial T2WI (TR/TE msec, 4250/97) also shows the moderate diffuse gray matter predominate cerebral volume loss and relative hypointensity of the thalami (arrows)



2015; Feraco et al. 2012) (Fig. 8.11). Vasculopathy and/or hemorrhages may occur at some point in the disease course, occasionally as the presenting symptom (Stefanits et al. 2014; Cohn et al. 2006). MRS shows decreased NAA, decreased choline, increased myoinositol, and/or increased glutamine and glutamate (Takeuchi et al. 2003; Holzbach et al. 1995).

### Neuronal Ceroid Lipofuscinosis (NCL)

This group of neurodegenerative disorders causes progressive cerebral and cerebellar cortical gray matter brain volume loss and white matter signal alteration (Whitehead and Gropman 2018) (Fig. 8.12). As with other lysosomal storage

disorders, thalamic hypointensity is also common, but an often overlooked feature (Autti et al. 2007). NAA may be decreased in keeping with neuronal loss (Bluml and Panigrahy 2013; Whitehead and Gropman 2018).

### Mucopolysaccharidoses (MPS)

Concurrent brain and bone abnormalities are key diagnostic features in MPS. Leukoencephalopathy with enlarged perivascular spaces is the most common brain manifestations (Barkovich and Patay 2019; Whitehead et al. 2015; Zafeiriou and Batziou 2013) (Fig. 8.13). Hydrocephalus is another frequent disease attribute. Dysostosis multiplex is found in the spine, commonly with craniocervical junction abnormalities

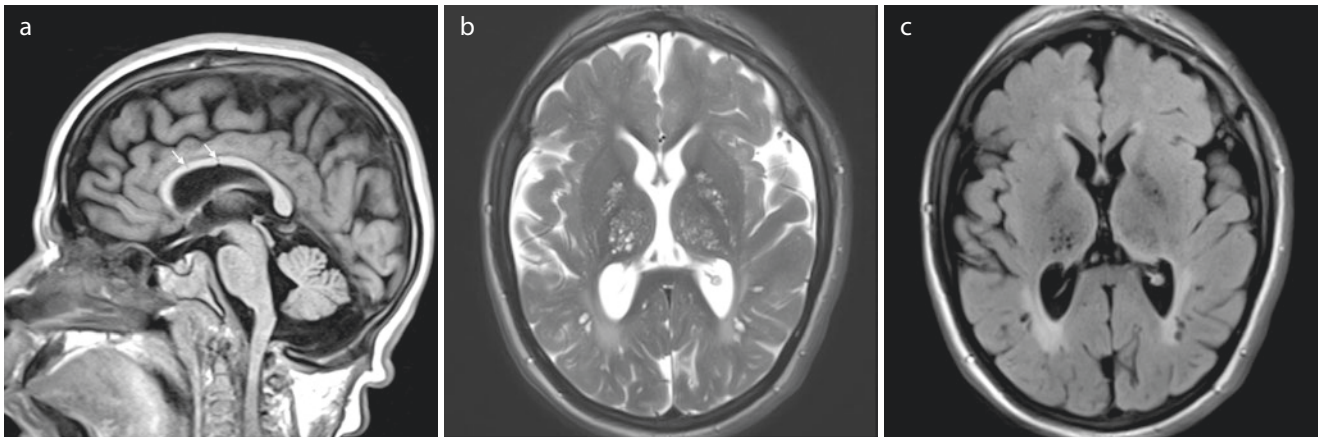


**Fig. 8.13** A 19-year-old male with mucopolysaccharidosis (Hunter syndrome). (a) Sagittal midline T1WI (TR/TE msec, 15/7) demonstrates skullbase and spinal hypoplasia/dysplasia with underdevelopment of the clivus, dysmorphic cervical vertebrae, and spinal/foramen magnum stenosis. The callosal genu and body are thin with small foci of hypointensity representing perivascular space enlargement (arrows).

and skull base dysplasia (Whitehead et al. 2015; Zafeiriou and Batziou 2013) (Fig. 8.13). MRS may demonstrate elevated myoinositol, increased glutamate, increased or decreased choline, decreased NAA, and/or abnormal lactate (Zafeiriou and Batziou 2013).

## Mitochondrial Disorders

**The mitochondrial respiratory chain disorders have a multisystem presentation and genetic origin. The combination of any symptom, organ or tissues, compounded with any age of presentation accounts for the challenge in diagnosing these conditions. From a neuroimaging standpoint, there are several hallmark features that when taken together with the clinical history should alert one to the possibility of these conditions. The more common disorders with characteristic imaging features are discussed below.**

### Leigh Disease

Leigh disease may be caused by a mitochondrial defect in a nuclear or mitochondrial gene and may have multiple organ system involvement. The most common presentation is the early infancy onset associated with severe neurodegeneration with encephalopathy, seizures, blindness, and progressive psychomotor regression typically resulting in death within 2–3 years, usually due to respiratory failure (Thorburn et al. 2003). MRI results in a distinctive brain disease characterized by variable signal changes in the basal ganglia, thalami, brainstem, and/or cerebellum with restricted diffusion ultimately evolving to combination of gliosis and necrosis

Hazy hypointense signal in the brainstem represents enlarged perivascular spaces. Axial T2WI (TR/TE msec, 3500/120) (b) and T2/FLAIR sequence (TR/TE/TI msec, 8000/82/2200) (c) reveal multiple prominent perivascular spaces in the white and deep gray matter (T2 hyperintense, FLAIR hypointense) on the background of FLAIR hyperintense white matter signal

(Whitehead and Gropman 2018; Whitehead et al. 2016) (Fig. 8.14). Arterial spin-labeling (ASL) perfusion sequence can show hyperperfusion in regions of active brain disease that may correspond to small vessel proliferation described on pathology (Whitehead et al. 2016) (Fig. 8.14). 1H MRS demonstrates elevated lactate in many cases; however, its absence does not exclude the disease.

### MELAS Syndrome

Mitochondrial encephalopathy with lactate acidosis and stroke-like episodes (MELAS) syndrome is typically of childhood onset characterized by stroke-like episodes, migraine, hearing loss, diabetes, and seizures. In those patients that survive into the late teens and early twenties, a severe gastroparesis is seen (Gagliardi et al. 2019). Characteristic brain lesions involve overlapping large vascular territories that help distinguish it from a non-metabolic thromboembolic infarction (Whitehead and Gropman 2018) (Fig. 8.15). Posterior predominant cortical and subcortical disease is typical, with progressive atrophy. The “black toenail sign” corresponding to gyral necrosis is a common neuroimaging finding associated with cerebral lesions of sufficient severity and chronicity (Whitehead et al. 2017a) (Fig. 8.15). Abnormal T2 FLAIR hyperintensity in and along cortical veins may predict disease severity and future development of brain lesions (Whitehead et al. 2017b) (Fig. 8.15). Deep gray nuclear mineralization is often present, though these structures may be spared of significant volume loss and focal lesions unlike in other mitochondrial diseases. MR spectroscopy shows elevated lactate most commonly at times of metabolic decompensation and may show reduced NAA in the setting of neuronal loss.



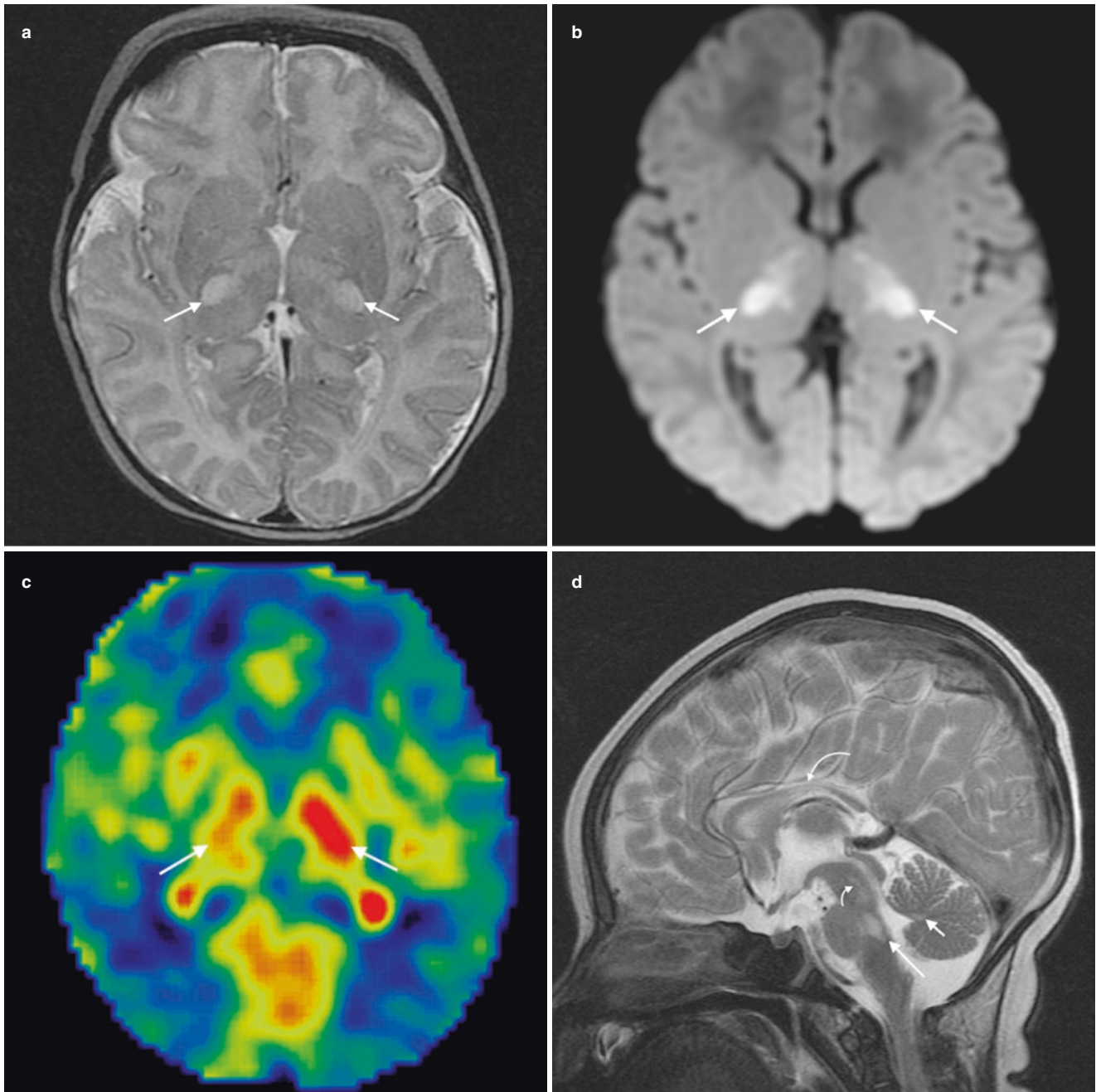


**Fig. 8.14** A 2-month-old female with Leigh disease due to a TRMU gene defect. (a) Axial T2WI (TR/TE msec, 3500/120) and (b) diffusion weighted image (TR/TE msec, 8000/85) at the level of the basal ganglia demonstrate T2 prolongation and reduced diffusion in the thalami (arrows). (c) The corresponding arterial spin labeling (ASL) perfusion sequence shows thalamic hyperperfusion (arrows). (d) Sagittal midline

T2WI (TR/TE msec, 3500/156) shows hyperintense lesions in the callosal body (long curved arrow), midbrain tegmentum (short curved arrow) pontine tegmentum (long straight arrow), and central vermis (short straight arrow). There is mild pontine hypoplasia and thinning of the corpus callosum

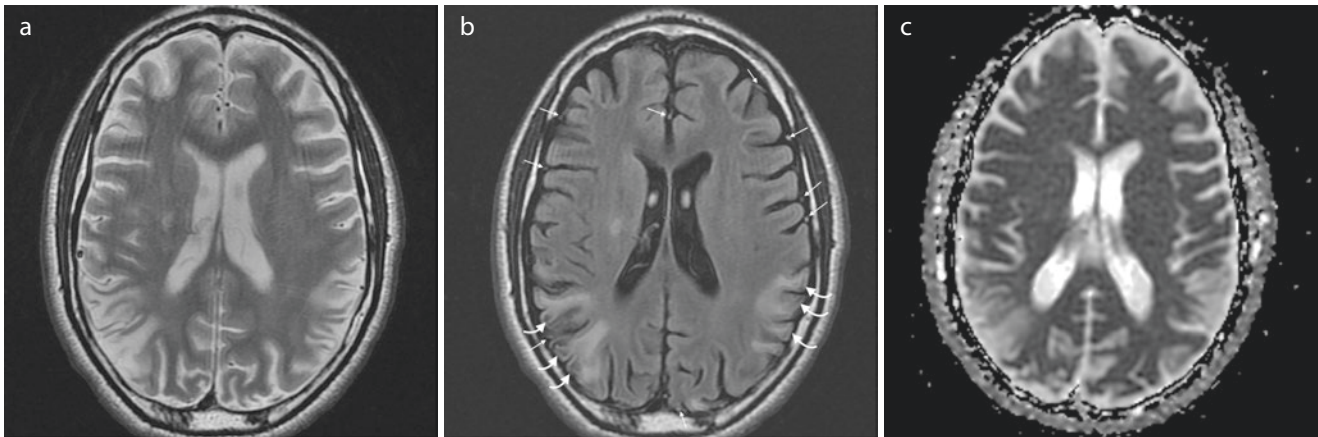


**Fig. 8.15** A 19-year-old male with MELAS. Axial T2WI (TR/TE msec, 3543/98) (a), T2 FLAIR (TR/TE/TI msec, 10,000/124/2200) (b), and apparent diffusion coefficient map (TR/TE msec, 10,000/95) (c) at the level of the lateral ventricles show bilateral parieto-occipital cortical/subcortical hyperintensity not confined to large arterial territories

with partial signal suppression superficially consistent with necrosis and the “black toenail” sign compatible with chronic MELAS-related brain injury (curved arrows, b). Note several cortical veins show FLAIR hyperintensity that may represent venopathy (straight arrows, b)

## White Matter Disorders/Leukodystrophies

**Leukodystrophy is one of a group of disorders characterized by degeneration of the white matter in the brain. Many are of genetic etiology due to IEMs (van der Knaap and Bugiani 2017). Leukodystrophies are often degenerative in nature, but some only impair white matter function. The clinical course may be static or progressive, but may also improve with time. Progressive leukodystrophies are often fatal. There has been a large increase in the number of genetically defined leukodystrophies in recent years due to recognition of magnetic resonance imaging patterns coupled with next-generation and whole exome sequencing (van der Knaap and Bugiani 2017).**

### X-linked Adrenoleukodystrophy (X-ALD)

The prototypical leukodystrophy for which there is significant MRI literature is X-ALD. The three recognizable clinical phenotypes are childhood cerebral disease, adrenomyeloneuropathy (AMN), and Addison disease. AMN manifests most commonly in an individual in his twenties or middle age with progressive lower extremity spastic weakness, sphincter disturbances, sexual dysfunction, and, often, impaired adrenocortical function. Addison disease only presents with primary adrenocortical insufficiency between age 2 years and adulthood and most commonly by age 7.5 years, usually without neurologic abnormality (Raymond et al. 1999). All are associated with elevation of very long chain fatty acids due to a mutation in the ABCD1 gene, which

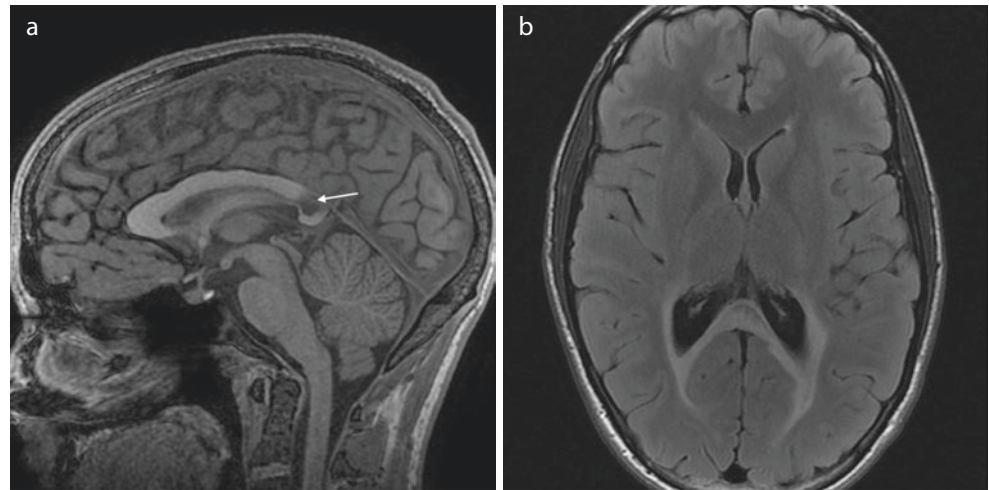
encodes for a peroxisomal very long chain fatty acid transporter.

The callosal splenium is usually the earliest and most commonly affected part of the brain in X-ALD (Barkovich and Patay 2019) (Fig. 8.16). Lesions quickly spread to the forceps major and, in worse cases, involve the projectional white matter fibers extending into the brainstem along with other brain white matter (Whitehead and Gropman 2018; Barkovich and Patay 2019; Loes et al. 1994). Laminated signal changes in the corpus callosum and adjacent commissural fibers are common in the subacute and chronic phases, reflecting multiple bouts of active brain disease and representing combined edema, inflammatory changes, and destructive changes (demyelination and necrosis). Therefore, the signal intensity is heterogenous and variable, often with mixed restricted diffusion and facilitated diffusion and variable contrast enhancement in the areas of active inflammation. Corticospinal tracts, visual, and auditory pathways are often involved. Loes score associated with lesion location and extent has been validated to determine brain disease severity and transplant candidacy (Loes et al. 1994). MRS is nonspecific, often depicting lactate, increased lipids, decreased NAA, and elevated choline (Bluml and Panigrahy 2013). However, an NAA:Cho less than 5 has been shown to predict clinical decline (Barkovich and Patay 2019).

### Zellweger Syndrome

Another peroxisomal-based disorder, Zellweger syndrome is a severe IEM with multisystemic manifestations. From a neurological standpoint, there is both gray and white matter

**Fig. 8.16** A 16-year-old male with X-linked adrenoleukodystrophy. (a) Sagittal midline T1WI (TR/TE msec, 8/3) demonstrates marked hypointensity within a mildly thinned callosal splenium (arrow). (b) Axial T2/FLAIR (TR/TE/TI msec, 10,000/144/2250) shows signal abnormality in the callosal splenium and forceps major with partial signal suppression in the splenium representing chronic demyelination/gliosis and necrosis



involvement. Neuroimaging findings are typified by cerebral polymicrogyria, often perisylvian predominant, caudothalamic groove germinolytic cysts, and white matter hyperintensity on T2WI (Whitehead et al. 2015) (Fig. 8.17). Germinolytic cysts carry a differential diagnosis of prior germinal matrix hemorrhage, TORCH infection, genetic, and toxic/metabolic disturbances (Herini et al. 2003). Significant hydrocephalus is unusual, unlike in the dystroglycanopathies. MRS can show elevated lipids associated with hepatic disease and decreased NAA (Bluml and Panigrahy 2013).

### Aicardi-Goutieres Syndrome (AGS)

Imaging manifestations in AGS are typified by leukoencephalopathy (diffuse or displaying an anteroposterior severity gradient), frontotemporal white matter rarefaction, reduced brain volume, and, importantly, parenchymal calcifications collectively overlapping with the appearance of some TORCH infections (La Piana et al. 2016; Vanderver et al. 2015) (Fig. 8.18). Brain malformations may include dysgenesis of the corpus callosum and/or cerebellar hypoplasia; however, malformations of cortical development are typically absent unlike in many cases of congenital CMV. Calcifications, a cornerstone feature, are generally detectable using certain gradient echo sequences; however, CT is more sensitive and may be required if the diagnosis is suspected, but no calcifications are found using MRI (La Piana et al. 2016). Central spinal cord signal hyperintensity has been described (Samanta and Ramakrishnaiah 2019). 1H MRS demonstrates reduced NAA and elevated MI (Robertson et al. 2004).

### Krabbe Disease

There are two main age-specific neuroimaging manifestations of Krabbe disease. In the infantile period, dentate hilar and basal ganglia signal abnormalities are present, whereas in later onset forms, a cerebral leukodystrophy with a posteroanterior (PA) and centrifugal gradient predominates often manifesting a “tigroid” pattern of signal alteration (Whitehead and Gropman 2018; Whitehead et al. 2015) (Fig. 8.19). The cerebral corticospinal tracts are often affected from the corona radiata to the cerebral peduncles. Cauda equina and cranial nerves (especially the optic pathway) may be thickened and show abnormal contrast enhancement. Deep cerebral white and gray matter mineralization is common; CT is useful for confirmation (Whitehead and Gropman 2018; Whitehead et al. 2015). MRS shows variable metabolic changes that may include elevated myoinositol and/or glutamate, increased or decreased choline, decreased NAA, and/or abnormal lactate (Bluml and Panigrahy 2013; Whitehead and Gropman 2018; Whitehead et al. 2015).

### Metachromatic Leukodystrophy (MLD)

Metachromatic leukodystrophy is an inherited disorder characterized by the accumulation of sulfatides. Sulfatide accumulation in myelin-producing cells causes progressive destruction of white matter throughout the nervous system, including the brain, spinal cord, and peripheral nerves. Imaging features of MLD are similar to Krabbe in



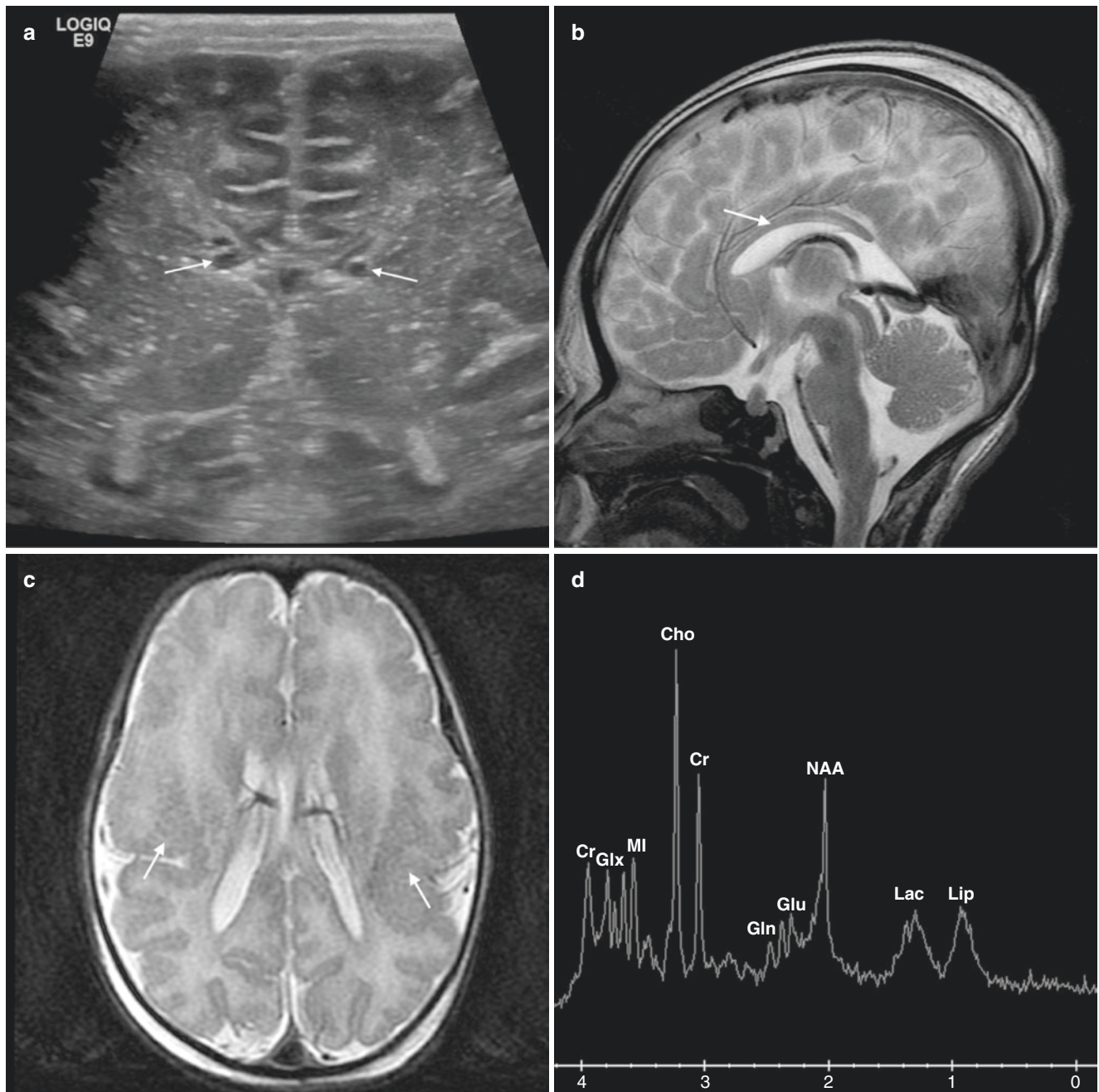
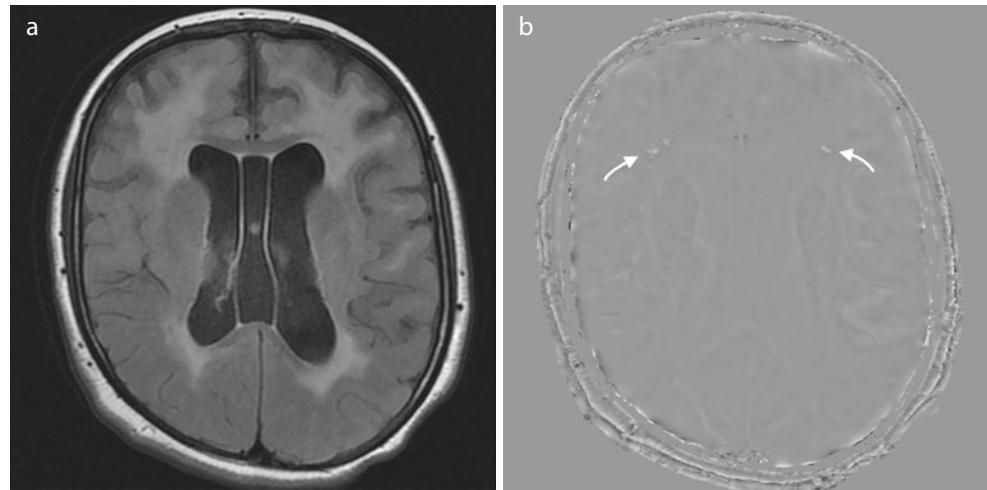


**Fig. 8.17** Neonatal female with Zellweger syndrome. (a) Coronal gray-scale head ultrasound shows bilateral caudothalamic groove germinolytic cysts (arrows). (b) Sagittal midline T2WI (TR/TE msec, 3500/158) shows mild thinning/dysmorphia of the corpus callosum consistent with hypogenesis/dysgenesis (arrow) and pontine hypoplasia. (c) Axial T2WI (TR/TE msec, 3500/120) through the lateral

ventricles depicts perisylvian predominant polymicrogyria (arrows). Short echo single voxel MRS over the left basal ganglia (TR/TE msec, 1500/35) (d) shows elevated lipids (Lip) and lactate (Lac), increased glutamine (Gln; Glx), and glutamate (Glu; Glx). NAA, Cr, and Cho ratios are borderline but within normal range



**Fig. 8.18** A 12-year-old female with Aicardi-Goutieres syndrome. (a) Axial T2 FLAIR (TR/TE/TI msec, 10,000/149/2200) MR image through the lateral ventricles shows anterior predominant white matter signal hyperintensity and ventriculomegaly reflecting cerebral volume loss. (b) The corresponding phase map from a susceptibility weighted sequence (SWAN; TR/TE msec, 38/23) shows bright dystrophic calcifications in the frontal subcortical white matter (arrows)



many ways including the tigroid cerebral white matter pattern, a PA and centrifugal gradient (in children), cranial nerve and cauda equina involvement, and elevated myo-inositol (Whitehead and Gropman 2018) (Fig. 8.20). Dentate nuclei tend to be spared and calcifications are absent, however.

### Canavan Disease

Aspartoacylase deficiency induced dysmyelination in Canavan disease causes diffuse spongiform thickening of the cerebral, cerebellar, and brainstem white matter with resultant macrocephaly in the infant brain (McAdams et al. 1990; Brismar et al. 1990). Neuroimaging shows swelling and widespread hyperintense white matter signal on T2WI often involving the thalami, globus pallidus, and cerebellar deep gray nuclei with relative sparing of the striatum (McAdams et al. 1990; Brismar et al. 1990) (Fig. 8.21). Sometimes the capsules, corpus callosum, and deep cerebellar white matter are also spared with more pronounced subcortical white matter involvement unlike in Krabbe and MLD. The absence of contrast enhancement and presence of restricted diffusion thought to represent water trapping associated with vacuolization helps distinguish Canavan from Alexander disease (Brismar et al. 1990; Sener 2004). Parenchymal volume loss may be present at diagnosis or develop over time; therefore macrocephaly is not universal (Brismar et al. 1990). MRS shows abnormally accumulated/elevated NAA, characteristic to the disease (Bluml and Panigrahy 2013) (Fig. 8.21). Milder juvenile forms of the disease have differing imaging changes including mild or absent leukodystrophy, striatum signal changes, and lack of NAA elevation (Toft et al. 1993; Nguyen and Ishak 2015).

### tRNA Synthetase Disorders

Brain disease in tRNA synthetase disorders includes leukodystrophy, hypomyelination, Leigh-like, and/or MELAS-like patterns with metabolic strokes; lactate may be present on MRS. AARS2, DARS2, and EARS2 are three of the most well-described gene defects with fairly specific imaging manifestations. In AARS2, a deep anterior frontal and posterior parietal leukodystrophy develops, relatively sparing frontoparietal junctional tissue but involving the corticospinal tracts, frontopontine, and parietooccipital pontine fibers (Dallabona et al. 2014). DARS2 genetic abnormalities cause leukoencephalopathy with brainstem and spinal cord involvement and lactate elevation (LBSL); the deep cerebral white matter is involved with or without a PA severity gradient, multiple brainstem white matter tracts are affected (corticospinal, spinocerebellar, medial lemniscus, cerebellar peduncles, and intraparenchymal trigeminal nerve fibers), and spinal cord signal changes are present (Kassem et al. 2014). In EARS2, neuroimaging patterns may include hypomyelination, deep cerebral leukodystrophy with relative periventricular sparing, and Leigh-like involvement of the thalamus, dentate nucleus, and dorsal brainstem (Steenweg et al. 2012).

### Substrate Depletion Disorders

**The more common disorders with substrate depletion are discussed below.**

### Creatine Deficiency Syndromes

The cerebral creatine deficiency syndromes are inborn errors of creatine metabolism that include the creatine biosynthesis disorders, guanidinoacetate methyltransferase (GAMT) defi-

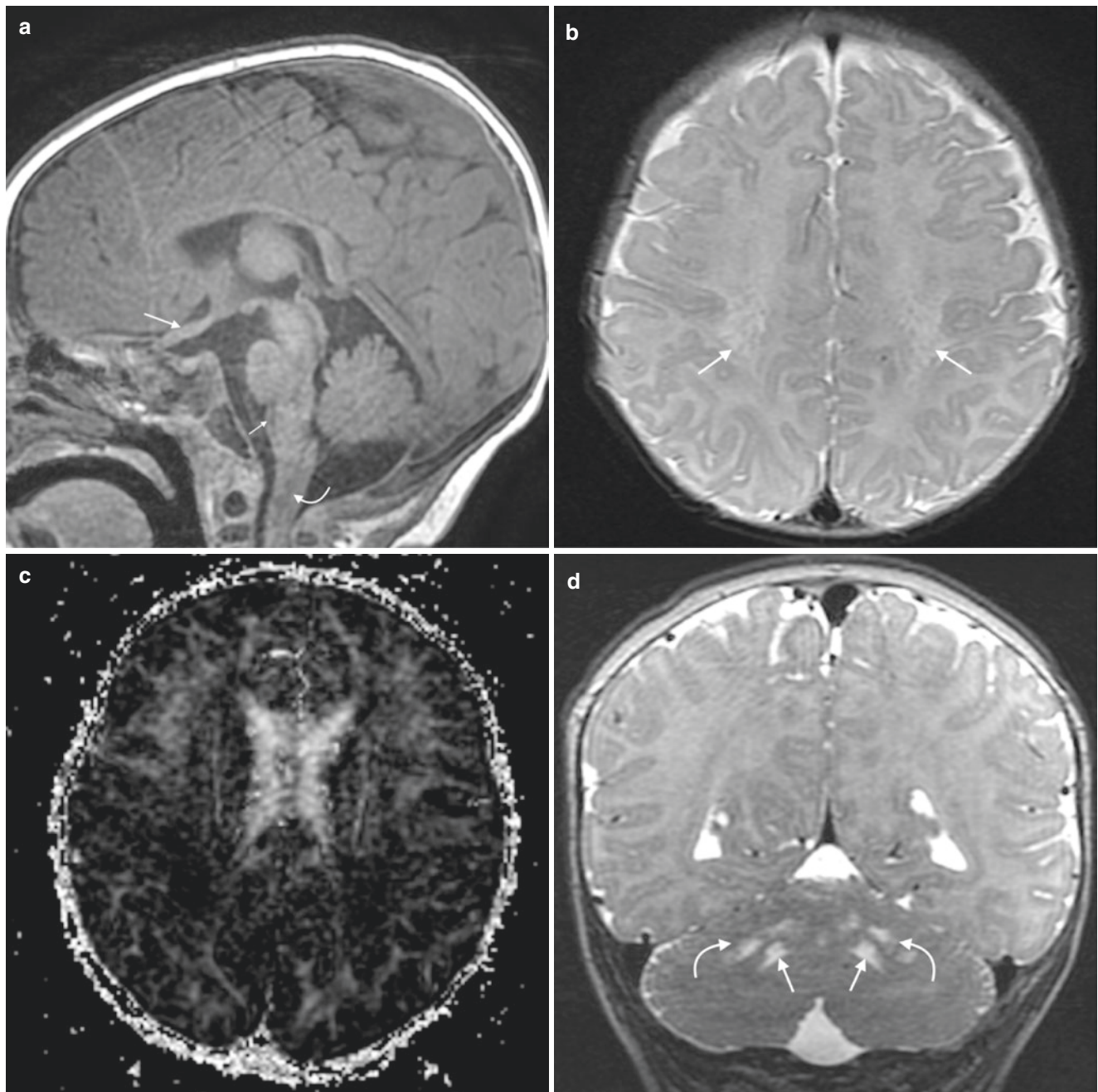


**Fig. 8.19** A 4-month-old male with Krabbe disease. (a) Sagittal midline T1WI (TR/TE msec, 8/3) shows thickening of the optic chiasm (large arrow), thickening of the medulla oblongata and hypointensity of the pyramidal tracts (small arrow), and thickening of the upper cervical spinal cord with abnormal hypointense signal (curved arrow). (b) Axial T2WI (TR/TE msec, 3500/90) at the level of the corona radiata depicts striated/tigroid deep frontoparietal white matter signal (arrows). (c)

DTI image (TR/TE msec, 10,000/92) at a slightly lower section of the cerebrum demonstrates a posterior to anterior gradient of diffused anisotropy with hypointense white matter. (d) Coronal T2WI (TR/TE msec, 3500/90) through the cerebellum shows abnormally increased signal in the dentate hila (straight arrows) and cerebellar white matter (curved arrows)

ciency, and L-arginine:glycine amidinotransferase (AGAT or GATM) deficiency, as well as the creatine transporter (SLC6A8) deficiency. All three are characterized by clinical presentation including seizures and intellectual disability, although behavioral difficulties such as autism spectrum and

an extrapyramidal movement disorder may be seen. Onset is between ages 3 months and 3 years. The phenotype of SLC6A8 deficiency in affected males ranges from mild intellectual disability and speech delay to significant intellectual disability, seizures, and behavioral disorder. GATM and



AGAT deficiency are autosomal recessive conditions, whereas the transport defect is an X-linked disorder (Gropman 2012). Apart from occasional periventricular white matter signal hyperintensity, structural imaging fails to disclose sig-

nificant abnormalities. MR spectroscopy is critical for the diagnosis and useful in follow-up by demonstrating reduced concentration of creatine compounds at 3 and 3.9 ppm (Whitehead and Gropman 2018) (Fig. 8.22) (Table 8.1).

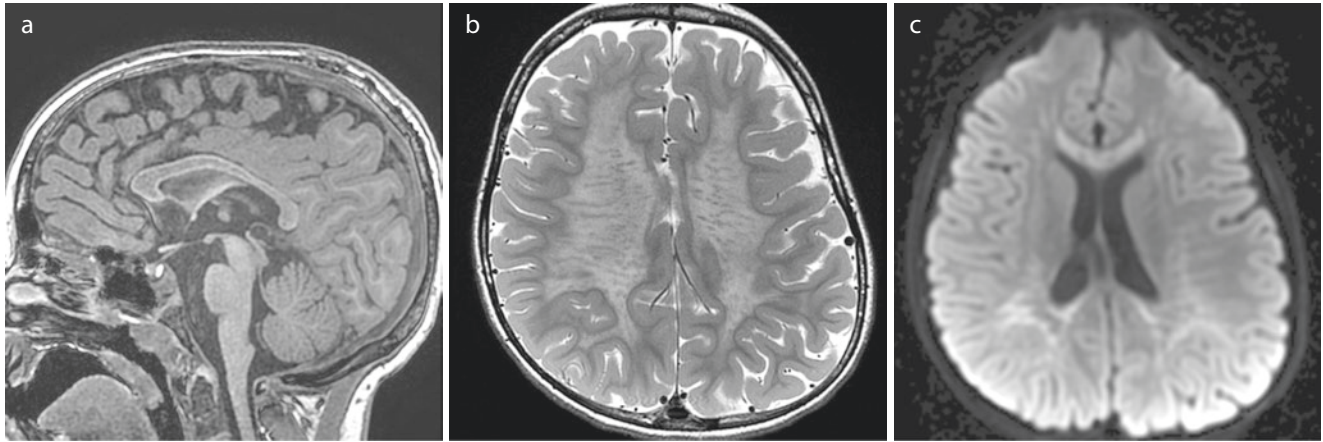


**Fig. 8.20** A 6-year-old female with metachromatic leukodystrophy. (a) Sagittal midline T1WI (TR/TE msec, 8/3) demonstrates extensive hypointense signal throughout most of the corpus callosum, sparing peripheral most fibers and some central fibers with a stippled appearance; the posterior fossa structures are normal. (b) Axial T2WI (TR/TE msec, 3205/102) at the level of the corona radiata depicts striated/

tigroid deep frontoparietal white matter signal. (c) Axial diffusion weighted image (TR/TE msec, 10,000/70) at a slightly lower section of the cerebrum demonstrates striated and confluent deep and periventricular white matter reduced diffusion consistent with intramyelinic edema

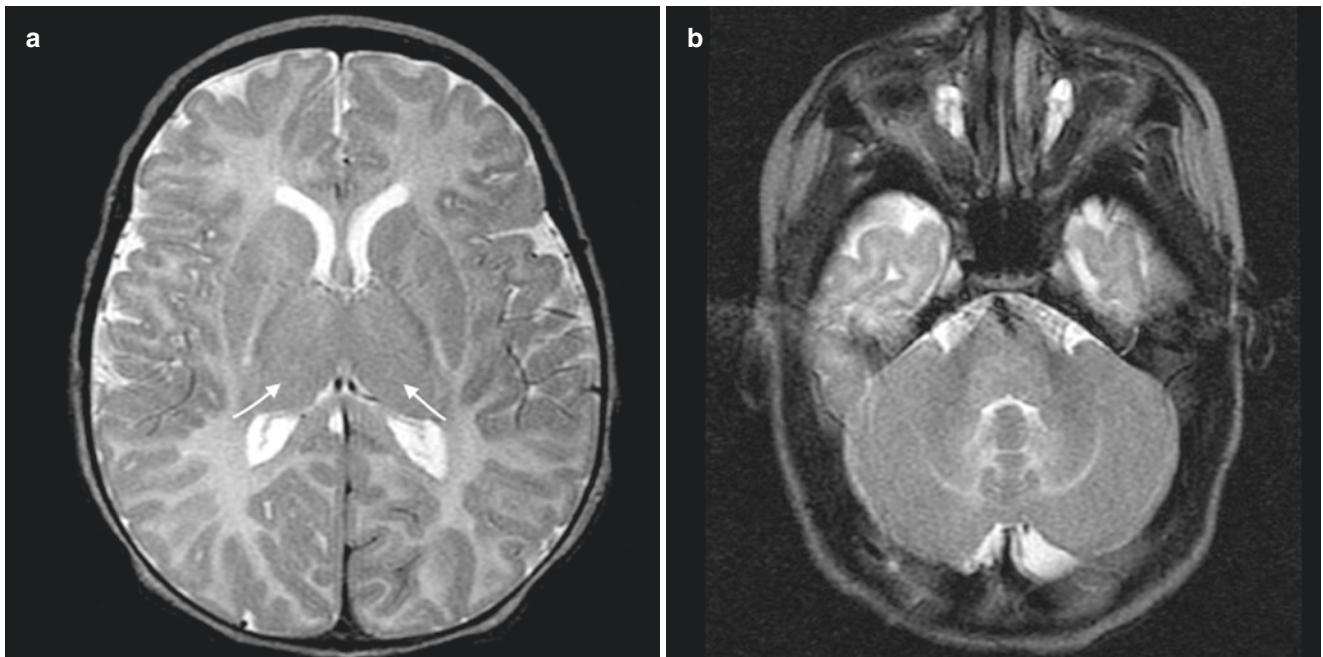


**Fig. 8.21** A 2-month-old female with Canavan disease. Axial T2WI (TR/TE msec, 3500/10) through the basal ganglia (a) and cerebellum (b) reveals generalized mild cerebral, cerebellar, and brainstem white matter hyperintensity for age and subtle increased signal in the thalami (arrows, a). (c) Axial diffusion weighted image (TR/TE msec, 7500/61)

through the basal ganglia hyperintense signal of the cerebral white matter and thalami representing reduced diffusion/intramyelinic edema; note sparing of the striatum. (d) Single voxel MRS over the left basal ganglia (TR/TE msec, 1500/35) shows abnormal NAA elevation (NAA), diagnostic of Canavan disease

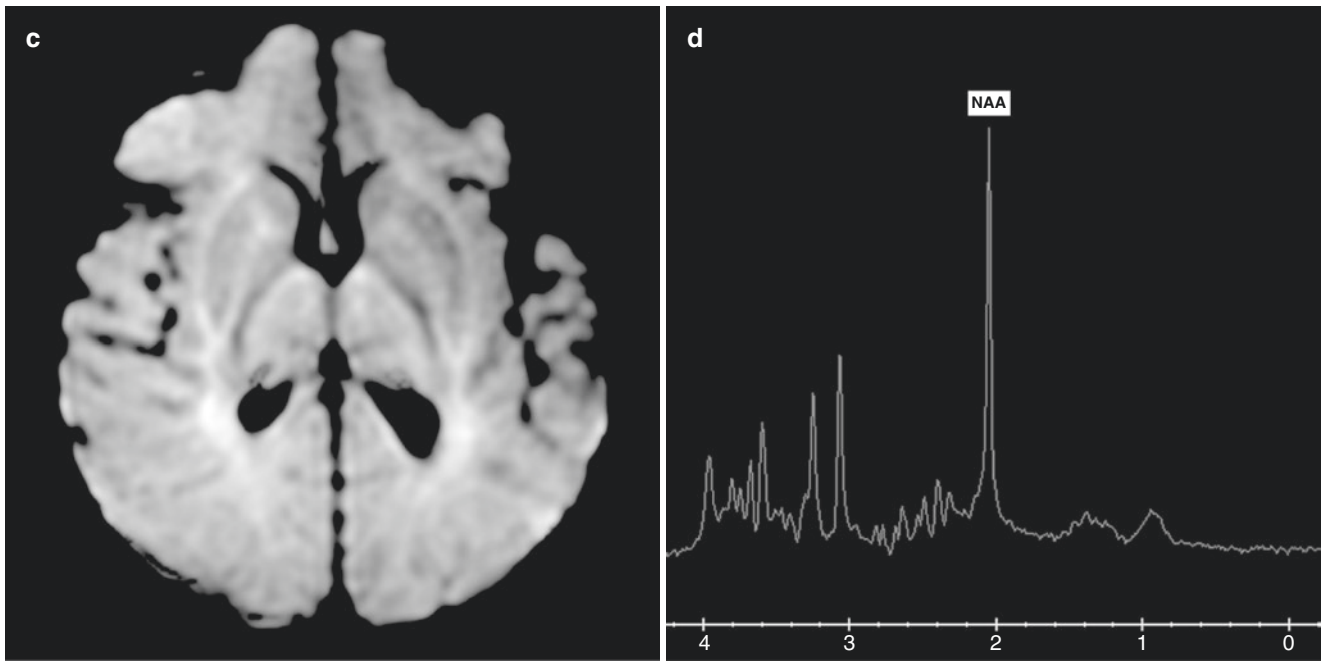


**Fig. 8.21** (continued)

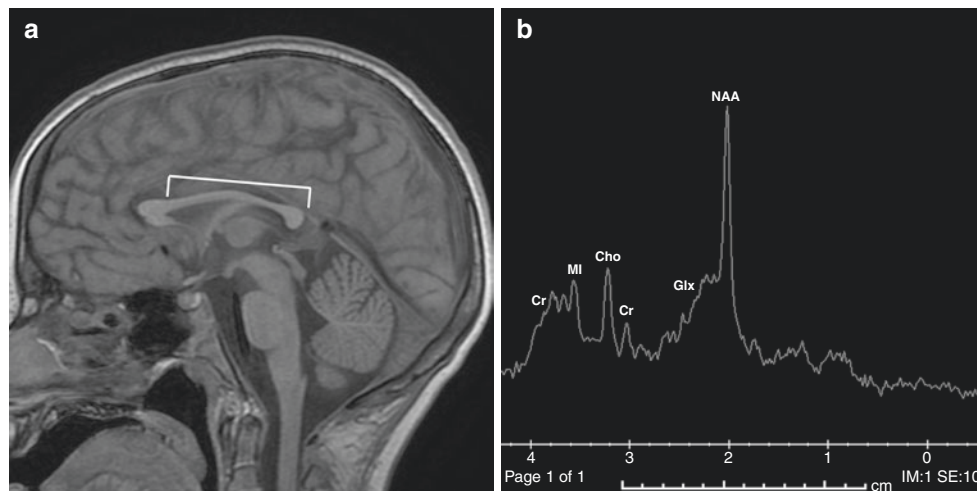


**Fig. 8.22** An 11-year-old male with X-linked creatine transporter deficiency secondary to a SLC6A8 gene defect. (a) Sagittal midline T1WI (TR/TE msec, 11/5) shows thinning of the body, isthmus, and genu of the corpus callosum representing mild posterior predominant cerebral white matter volume loss without signal alterations (bracket). (b) Single

voxel MRS over the left basal ganglia (TR/TE msec, 1500/35) shows marked reduction of creatine compounds (Cr) at 3 and 3.9 ppm; other metabolites including *N*-acetylaspartate (NAA), glutamine and glutamate (Glx), choline (Cho), and myoinositol (MI) are normal



**Table 8.1** This table was constructed after a thorough review of existing medical literature and is arranged consecutively by chapter. Brain/spine MR imaging patterns were compiled based on lesion location within the cerebrum, cerebellum, brainstem, and/or spinal cord, texture (signal changes on different sequences), volume, concurrent malformations, and other manifestations for each disease process. The range of reported brain MRS alterations was also documented. Diseases with normal or nonspecific imaging patterns were excluded. We emphasize that the current medical literature does not accurately reflect the entire imaging spectrum of all metabolic disease phenotypes. Therefore, the information in this table should be considered dynamic and no more than a loose guideline. We hope that this information will be elaborated upon and altered when it becomes necessary to enhance specificity as new data comes to light in the future

Chapter	Disease	Prevailing pattern(s)	Cerebrum			Cerebellum			Brainstem			Spinal cord	Malformations and other findings	MRS (ppm)	
			Location	Texture	Volume	Location	Texture	Volume	Location	Texture	Volume				
13.11	Adenylosuccinate lyase deficiency	Hypomyelination	cortex: n	DWI: ?	↓-n	cortex: n	DWI: ?	↓-n	mb: n	DWI: ?	↓-n	?	-	Succinyladenosine (8.3)	
			wmsc: +	T2: ↑		wmsc: +	T2: ↑		pons: n	T2: ↑				Succinylaminimidazole carboxamide riboside (7.5)	
13.14	Adenosine monophosphate deaminase 2 deficiency	PCH CCD	n	n	↓	n	n	↓-↓	n	n	↓-↓-↓-↓	?	ACC, HCC, CCD PCH	?	
13.17	Adenosine deaminase 2 deficiency	Midbrain "figure of 8" sign													
		Lacunar infarcts	cortex: +/-	DWI: +/-	↓-n	n	n	n	mb: +/-	DWI: +/-	n	?	SDH +/-		
14.11	Aicardi-Goutières syndrome (ACG) and ACG-like (Shared features)	Vasculopathy	wmsc: +/-	T2: ↑-n					pons: +/-	T2: ↑-n			IVH +/-		
			wmd: +/-	myelin: n					med: +/-	myelin: n			COW stenoses/occlusions +/-		
14.1-	Alcadi-Goutières syndrome (ACG) and ACG-like (Shared features)	Calcifications	BG: +/-	Nec: -											
		Leukoencephalopathy (diffuse or anteroposterior gradient with frontotemporal white matter rarefaction)	Thal: +/-	Ca: -						Ca: -					
14.11	Aicardi-Goutières syndrome (ACG) and ACG-like (Shared features)	Atrophy		Hem: +/-											
			cortex: n	DWI: -	n-↓↓↓	cortex: n	DWI: +/-	n-↓↓↓	mb: +/-	DWI: +/-	n-↓	↑T2 central +/-	Cerebellar hypoplasia +/-	NAA ↓	
15.2	Guanidinoacetate methyltransferase deficiency (cerebral Cr deficiency syndrome type 2)	Leukoencephalopathy	wmsc: ++	T2: ↑-↑↑					pons: +/-	T2: ↑			HCC +/-	MI ↑	
			wmd: ++	myelin: ↓											
15.2	Guanidinoacetate methyltransferase deficiency (cerebral Cr deficiency syndrome type 2)	Globus pallidus hyperintensity	BG: ++	Nec: +/-											
			Thal: +	Ca: +++											
15.3	Creatine transporter deficiency (cerebral Cr deficiency syndrome type 1)	MRS: Cr reduction	cortex: n	DWI: -	↓-n	n	n	mb: +/-	DWI: +/-	n	?	-		Cr ↓ to absent	
			wmsc: n	T2: ↑-n				pons: +/-	T2: ↑-n					Guanidinoacetate (3.8)	
15.3	Creatine transporter deficiency (cerebral Cr deficiency syndrome type 1)		wmd: n	myelin: n											
			BG: ++	Nec: -											
15.3	Creatine transporter deficiency (cerebral Cr deficiency syndrome type 1)		Thal: n	Ca: -											
			cortex: n	DWI: -	↓-n	n	n	n	n	n	?	-		Cr ↓ to absent	
15.3	Creatine transporter deficiency (cerebral Cr deficiency syndrome type 1)		wmsc: n	T2: ↑-n											
			wmd: +/-	myelin: n											
15.3	Creatine transporter deficiency (cerebral Cr deficiency syndrome type 1)		BG: n	Nec: -											
			Thal: n	Ca: -											
15.3	Creatine transporter deficiency (cerebral Cr deficiency syndrome type 1)			CE: ?											
			cortex: n	DWI: -	↓-n	n	n	n	n	n	?	-		Cr ↓ to absent	

(continued)

Table 8.1 (continued)

Chapter	Disease	Prevailing pattern(s)	Cerebrum			Cerebellum			Brainstem			Spinal cord	Malformations and other findings	MRS (ppm)
			Location	Texture	Volume	Location	Texture	Volume	Location	Texture	Volume			
17.2	Carbamoylphosphate synthetase I deficiency	Diffuse cerebral edema/injury Central cerebral predominant injury pattern sparing thalami Metabolic stroke	cortex: ++	DWI: +/-	n-↓↓↓	n	n	n	n	n	n	?	-	Glx ↑
			wmsc: ++	T2: ↑↑↑↑										
17.3	Ornithine transcarbamylase deficiency	Diffuse cerebral edema/injury Central cerebral predominant injury pattern sparing thalami Metabolic stroke	wmd: ++	myelin: n										NAA n-↓
			BG: ++ Thal: +/-	Nec: +/- Ca: - CE: ?										
17.4	Argininosuccinate synthetase deficiency	Central cerebral predominant injury pattern sparing thalami Diffuse cerebral edema/injury Metabolic stroke	cortex: ++	DWI: +/-	n-↓↓↓	n	n	n-↓	n	n	n	?	-	Glx ↑
			wmsc: ++	T2: ↑↑↑↑										
17.5	Argininosuccinate lyase deficiency	Central cerebral predominant injury pattern sparing thalami Diffuse cerebral edema/injury Metabolic stroke	wmsc: ++	T2: ↑↑↑↑										MI ↓ NAA n-↓
			wmd: ++ BG: ++ Thal: +/-	myelin: n Nec: - Ca: - CE: ?										
17.6	Arginase deficiency	Central cerebral predominant injury pattern sparing thalami MRS: arginine	cortex: +/-	DWI: +/-	↓-n	n	n	n	n	n	n	?	Heterotopia	Guanidinoacetate (3.8)
			wmsc: +/- wmd: +/- BG: +/- Thal: n	T2: n-↑↑ myelin: n Nec: - Ca: - CE: ?										
17.6	Arginase deficiency	MRS: arginine	cortex: +/-	DWI: +/-	↓-n	n	n	↓-n	n	n	n	?	-	Arginine (3.8) NAA n-↓
			wmsc: +/- wmd: +/- BG: +/- Thal: n	T2: n-↑↑ myelin: n Nec: - Ca: - CE: ?										

17.17	Pyruvate carboxylase deficiency	Periventricular cysts/cystic necrosis Temporopolar white matter rarefaction	cortex: n	DWI: ?	n-↓↓	cortex: n	DWI: ?	n	mb: +/-	DWI: ?	n	?	SDH +/-	Lactate
			wmsc: +/-	T2: ↑↑		wmsc: +/-	T2: ↑-n		pons: +/-	T2: ↑-n				
20.1	Phenylalanine hydroxylase deficiency	PVWM involvement MRS: Phe	wmd: +/-	myelin: ↓		wmd: +/-	myelin: ↓-n		med: +/-	myelin: ↓-n				Cho ↑
			BG: n	Nec: ++		DN: n	Nec: -							
			Thal: n	Ca: -		Ca: -	Ca: -			Ca: -				
				CE: ?			CE: ?			CE: ?				
				hem: +/-			hem: +/-			hem: -				
			cortex: n	hem: +/-	n	n	n	n	n	n	n	n	-	Phe (7.3-7.4)
			wmsc: +/-	T2: ↑↑↑										
			wmd: +++	myelin: n										
			BG: n	Nec: -										
			Thal: n	Ca: +/-										
				CE: ?										
20.4	Dihydropyridine reductase deficiency	Leukodystrophy, cerebrum	Cortex: +/-	DWI: ?	n-↓↓	n	n	↓-n	-	n	n	n	-	?
			wmsc: +++	T2: ↑↑↑										
			wmd: +++	Myelin: n										
			BG: +/-	Nec: +										
			Thal: n	Ca: ++										
				CE: ?										
21.2, 21.3	Tyrosinemia	Globus pallidus lesions Intramylaric edema	cortex: n	DWI: ++	n	n	n	n	n	n	n	n	-	?
			wmsc: +/-	T2: ↑										
			wmd: +/-	Myelin: n										
			BG: ++	Nec: -										
			Thal: n	Ca: -										
				CE: ?										
22.6	Cystathionine β-synthase deficiency (classic homocystinuria)	Transient intramylaric edema diffuse cerebral white matter Venous thromboses +/- venous infarct Arterial thrombosis +/- arterial infarct	cortex: +/-	DWI: +/-	n-↓↓↓	n	n	n-↓	n	n	n	n	Sinus thrombosis +/-	Cho ↓-n-↑
			wmsc: +/-	T2: ↑										
			wmd: +/-	Myelin: n									Arterial thrombosis +/-	
			BG: n	Nec: -									Ectopic lens +/-	
			Thal: n	Ca: -									Hydrocephalus +/-	
				CE: ?										
				Hem: +/-										

(continued)













Table 8.1 (continued)

Chapter	Disease	Prevailing pattern(s)	Cerebrum			Cerebellum			Brainstem			MRS (ppm)
			Location	Texture	Volume	Location	Texture	Volume	Location	Texture	Volume	
31.1	Thiamine transporter 2 deficiency (biotine and thiamine responsive basal ganglia disease)	Leigh-like	cortex: +/-	DWI: +/-	↑-n-↓	cortex: +/-	DWI: +/-	↑-n-↓	mb: +/-	DWI: +/-	↑-n-↓	Lactate +/-
		Wernicke encephalopathy-mimic	wmsc: +/-	T2: ↑↑	↓↓	wmsc: +/-	T2: n-↑		p: +/-	T2: n-↑		Pyruvate (2.4) +/-
31.3	Thiamine pyrophosphokinase deficiency	Leigh-like	wmd: +/-	Myelin: n		wmd: +/-	Myelin: n		mi: +/-	Myelin: n		NAA n-↓
			BG: +/-	Nec: +/-		D: +/-	Nec: -					Cho n-↑
31.4	Mitochondrial thiamine pyrophosphate transporter deficiency	Severe brain hypoplasia and pachygyria/lisencephaly (amish lethal microcephaly)	cortex: n	DWI: ?	n-↓	cortex: n	DWI: ?	n	mb: +/-	DWI: ?	n	?
		Medullary and/or MCP lesions	wmsc: +/-	T2: ↑		wmsc: +/-	T2: ↑		p: +/-	T2: n-↑		
32.1-32.2	Riboflavin transporter deficiency (Brown-Vialetto-van Laere syndrome)	Severe brain hypoplasia and pachygyria/lisencephaly (amish lethal microcephaly)	wmd: +/-	Myelin: ↓		wmd: +/-	Myelin: n		mi: +/-	Myelin: n		
		DC spinal cord SA	BG: ++	Nec: +/-		D: ++	Nec: -					
32.6-32.7	Electron transfer flavoprotein subunit or dehydrogenase deficiency (glutaric aciduria type 2)	Intramyelinic edema cerebellum and/or cerebellum	n	n	↓↓	n	n	↓↓↓	n	n	↓↓↓	Brain hypoplasia; pachygyria/lisencephaly; malformed deep gray nuclei
		Temporal hypoplasia	n	n	n	n	n	n	mb: n	DWI: -	n-↓	Optic atrophy +/-
32.6-32.7	Electron transfer flavoprotein subunit or dehydrogenase deficiency (glutaric aciduria type 2)	Intramyelinic edema cerebellum and/or cerebellum	cortex: n	DWI: +/-	n-↓	cortex: n	DWI: +/-	n	n	n	n	Lactate
		Temporal hypoplasia	wmsc: +/-	T2: n-↑		wmsc: +/-	T2: n-↑		p: +/-	T2: n-↑		Optic nerve hypertense T2 +/-
32.6-32.7	Electron transfer flavoprotein subunit or dehydrogenase deficiency (glutaric aciduria type 2)	Frontal hypoplasia +/-	wmd: +/-	Myelin: +/-		wmd: +/-	Myelin: n		mi: +/-	Myelin: n		MCPhyperintensity +/-
		MCPhyperintensity +/-	BG: +/-	Nec: -		D: n	Nec: -					Thick CC +/-
32.6-32.7	Electron transfer flavoprotein subunit or dehydrogenase deficiency (glutaric aciduria type 2)	Frontal hypoplasia +/-	Thal: n	Ca: -		Thal: n	Ca: -					Thick CC +/-
		MCPhyperintensity +/-	Thal: n	Ca: -		Thal: n	Ca: -					Thick CC +/-

33.9	Pantothenate kinase 2 deficiency	"Eye of the tiger" sign	cortex: n	DWI: -	n-↓↓	cortex: n	DWI: +/-	n-↓↓↓	mb: +/-	DWI: -	n-↓↓↓	?	Optic atrophy +/-	NAA ↓
			wmsc: +/-	T2: ↑↑		wmsc: +/-	T2: ↓-n-↑	p: n	T2: n-↓					
33.11	Coenzyme A synthase deficiency	"Eye of the tiger" sign	wmd: +/-	Myelin: n-↓		wmd: +/-	Myelin: n		m: n	Myelin: n				
			BG(gp): +++	Nec: +		D: +/-	Nec: -							
34.1	α-aminoacidic semialdehyde dehydrogenase deficiency	CC malformation Brain underdevelopment or malformation	Thal: n	Ca: +/-		Thal: n	Ca: -			Ca: -				
				CE: -		CE: -					CE: -			
35.1-35.3	Molybdenum cofactor deficiency	Cystic encephalomalacia PCH	cortex: n	DWI: +/-	n-↓↓↓	cortex: n	DWI: -	n-↓↓	mb: +/-	DWI: +/-	n-↓↓↓	?	ACC, CCD, HCC +/- MCD, heterotopia +/-	Lactate
			wmsc: +/-	T2: n-↑		wmsc: +/-	T2: n-↑	p: n	T2: n-↑					
36.1	Copper-transporting ATPase β subunit deficiency (Wilson disease)	Mixed T2 signal cerebral deep gray and midbrain Dentorubrothalamic tract involvement T1 shortening BG +/- midbrain Clausstrum T2 hyperintensity	wmd: +/-	Myelin: n-↓		wmd: +/-	Myelin: n		m: n	Myelin: n				Cho n-↑
			BG: ++	Nec: ++		D: +/-	Nec: -							MI n-↓
			Thal: +/-	Ca: +/-		Thal: +/-	Ca: -			Ca: -				Cr n-↓
				CE: -			CE: -							
				Hemi: +/-			Hemi: +/-							
			cortex: +/-	DWI: +/-	n-↓↓↓	cortex: n	DWI: -	n-↓↓	mb: +/-	DWI: +/-	n-↓↓	"Bullet shaped" vertebral dysplasia +/-	HCC, CCD +/-	Lactate +/-
			wmsc: +/-	T2: ↓-n-↑		wmsc: n	T2: ↓-n-↑		p: +/-	T2: ↓-n-↑				NAA n-↓
			wmd: +/-	T1: ↓-n-↑		wmd: +/-	T1: ↓-n		m: +/-	T1: ↓-n-↑				Cho ↓-n-↑
			BG: +/-	Myelin: n		D: +/-	Myelin: n			Myelin: n				MI n-↓
			Thal: +/-	Nec: +/-		Thal: +/-	Nec: -			Nec: -				Lipids n-↑
				Ca: +/-			Ca: +/-			Ca: -				Cr n-↓
				CE: +/-			CE: -			CE: -				

(continued)

Table 8.1 (continued)

Chapter	Disease	Prevaling pattern(s)	Cerebrum	Cerebellum	Brainstem	Spinal cord	Malignancies and other findings	MRS (ppm)
36.2	Copper-transporting ATPase $\alpha$ subunit deficiency (Menke disease)	Tortuous, elongated arteries	Location cortex: +/-	Volume ↑-n ↓↓↓	Location cortex: n	Texture DWI: -	Volume n-↓↓	
		Delayed myelination Basal ganglia lesions	wmsc: +/- wmd: +/-	Texture T2: n-↑↑ Myelin: n-↓	wmsc: n wmd: +/-	Texture T2: n-↑ Myelin: n	Texture DWI: - T2: n-↑ Myelin: n	Tortuous, elongated arteries Dural sinus ectasia +/- SDH +/-
37.1–37.5	Hereditary hemochromatosis	Infantile transient temporal lobe tumefactive edema SDH	Location Thal: +/-		Location D: n	Texture Nec: +/-		
		Deep gray nuclear iron deposition	cortex: n wmsc: +/- wmd: +/- BG: +++ Thal: +/-	Volume n-↓	cortex: n wmsc: n wmd: n D: ++ Myelin: n Nec: - Ca: - CE: -	Location mb: +/-	Texture DWI: - T2: ↓ T1: n-↑ Myelin: n Nec: - Ca: - CE: -	Volume n
37.7	Ferritin light chain superactivity (neuroferritinopathy)	Widespread gray matter iron deposition +/- necrosis	cortex: +	Volume n-↓	cortex: +/-	Texture DWI: -	Volume n-↓	
		“Eye of the tiger” sign	wmsc: n wmd: n BG: +++ Thal: +/-	Texture T2: ↓-↑ T1: n-↑ Myelin: n Nec: +/- Ca: - CE: -	Location p: n m: n	Texture T2: ↓-↑ T1: n Myelin: n Nec: +/- Ca: - CE: -	Volume n-↓	?
37.8	Hereditary ceruloplasmin deficiency	Widespread homogeneous gray matter iron deposition	cortex: +	Volume n-↓	cortex: +/-	Texture DWI: -	Volume n-↓	
		Necrosis unusual	wmsc: n wmd: n BG: ++ Thal: +/-	Texture T2: ↓ T1: n Myelin: n Nec(thal): +/- Ca: - CE: -	Location p: n m: n	Texture T2: ↓ T1: n Myelin: n Nec: - Ca: - CE: -	Volume n-↓	?

38.1	Hypermanganesemia with dystonia type 1	T1 ↑ BG, BS, deep cerebellum	cortex: n wmse: n wmd: n BG: +++ Thal: +/-	DWI: n T2: ↓ T1: ↑↑ Myelin: n Nec: - Ca: - CE: -	n	cortex: n wmse: n wmd: +/- D: +	DWI: - T2: n T1: ↑ Myelin: n Nec: - Ca: - CE: -	n	mb: + p: +/- m: n	DWI: - T2: n T1: ↑ Myelin: n Nec: - Ca: - CE: -	n-↓	? Pituitary T1↑ +/-	?
38.2	SLC39A14 deficiency	T1 ↑ BG and brain white matter	cortex: n wmse: + wmd: + BG: ++ Thal: n	DWI: n T2: ↓ T1: ↑↑ Myelin: n Nec: - Ca: - CE: -	n-↓	cortex: n wmse: + wmd: + D: +	DWI: - T2: ↓ T1: ↑ Myelin: n Nec: - Ca: - CE: -	n-↓	mb: + p: + m: n	DWI: - T2: n T1: ↑ Myelin: n Nec: - Ca: - CE: -	n-↓	T1 ↑ Pituitary T1↑ +/-	?
38.3	SLC39A8 deficiency	Leigh-like	cortex: n wmse: n wmd: n BG: ++ Thal: +/-	DWI: +/- T2: ↑↑ Myelin: n Nec: - Ca: - CE: -	n-↓	cortex: n wmse: +/- wmd: +/- D: +/- Thal: n	DWI: - T2: n-↓ T1: ↓-n-↓ Myelin: n-↓ Nec: - Ca: - CE: -	n	n n-↓	n n-↓	n-↓	?	?
39.11-39.13	Galactosemia	MRS: Galactitol	cortex: +/- wmse: +/- wmd: +/- BG: +/- Thal: n	DWI: +/- T2: n-↓ T1: ↓-n-↓ Myelin: n-↓ Nec: - Ca: - CE: -	n-↓	cortex: n wmse: +/- wmd: +/- D: +/- Thal: n	DWI: - T2: n-↓ T1: n-↓ Myelin: n-↓ Nec: - Ca: - CE: -	n-↓	mb: +/- p: +/- m: +/-	DWI: - T2: n-↓ Myelin: n Nec: - Ca: - CE: -	n	AC +/- Galactitol (3.7) NAA n-↓ MI n-↓ cho n-↓	?
39.18	Glucose-6-phosphate transporter deficiency	Hypoglycemic brain injury pattern Moyamoya	cortex: +/- wmse: +/- wmd: +/- BG: n Thal: n	DWI: +/- T2: n-↓ Myelin: n Nec: +/- Ca: - CE: ?	n-↓	cortex: +/- wmse: +/- wmd: +/- D: +/- Thal: n	DWI: - T2: n-↓ Myelin: n Nec: - Ca: - CE: -	n	n n-↓	n n-↓	n	Moyamoya +/-	?
39.21	Glycogen branching enzyme deficiency	Leukodystrophy CST and ML SA SC atrophy	cortex: n wmse: + wmd: ++ BG: n Thal: n	DWI: +/- T2: ↑ Myelin: n-↓ Nec: - Ca: - CE: -	↓	cortex: +/- wmse: +/- wmd: +/- D: +/- Thal: n	DWI: - T2: n-↓ Myelin: n Nec: - Ca: - CE: -	↓	mb: + p: + m: +	DWI: - T2: ↑ Myelin: n Nec: - Ca: - CE: -	↓	Marked diffuse atrophy DC T2↑ +/-	NAA ↓ Lactate

(continued)













Table 8.1 (continued)

Chapter	Disease	Prevailing pattern(s)	Cerebrum			Cerebellum			Brainstem			Spinal cord	Malformations and other findings	MRS (ppm)
			Location	Texture	Volume	Location	Texture	Volume	Location	Texture	Volume			
44.49	UQCRQ deficiency	Leigh-like	cortex: n wmse: n wmd: n BG: ++ Thal: n	DWI: ? T2: ↑↑ Myelin: n Nec: + Ca: - CE: ?	↓	n	n	n	n	n	?	-	?	
44.52	TTIC19 deficiency	Leigh-like	cortex: n wmse: n wmd: n BG: +/- Thal: n	DWI: +/- T2: n-↑↑ Myelin: n Nec: +/- Ca: - CE: ?	n-↓	n	n-↓	mb: +/- p: n m: +/-	DWI: ? T2: n-↑ Myelin: n Nec: - Ca: - CE: ?	n	n	Vermian hypoplasia +/-	Lactate +/-	
44.54	LYRM7 deficiency	Cavitating leukodystrophy, patchy cerebral wm lesions Spinal cord SA	cortex: n wmse: +/- wmd: ++ BG: n Thal: +/-	DWI: +/- T2: ↑-↑↑ Myelin: n-↓ Nec: + Ca: - CE: +/-	n-↓	cortex: n	wmse: +/- wmd: +/-	mb: +/- p: +/- m: ++	DWI: ? T2: n-↑ Myelin: n Nec: - Ca: - CE: ?	n-↓	n-↓	SCSA +/-	Optic chiasm T2 hyperintensity	?
44.55	Cytochrome c oxidase subunit I deficiency	Leigh-like	cortex: n wmse: n wmd: n BG: ++ Thal: n	DWI: +/- T2: ↑↑ Myelin: n Nec: + Ca: - CE: ?	n	n	n	n	n	n	?	-	?	
44.60	Cytochrome c oxidase subunit 6B1 deficiency	Cavitating leukodystrophy, deep cerebrum	cortex: n wmse: +/- wmd: +++ BG: n Thal: n	DWI: +/- T2: ↑↑ Myelin: n Nec: + Ca: - CE: ?	↓-↓	n	n	n	n	n	n	?	-	?
44.75	SURF1 deficiency	Leigh-like HOD STN lesions, cerebral deep gray nuclei often spared	cortex: n wmse: n wmd: +/- BG: +/- Thal: +/-	DWI: +/- T2: n-↑↑ Myelin: n-↓ Nec: +/- Ca: - CE: -	n-↓	cortex: n wmse: +/- wmd: +/-	DWI: ? T2: n-↑↑ Myelin: n	mb: +/- p: +/- m: +/-	DWI: +/- T2: n-↑↑ Myelin: n	n-↓	Cervical T2↑	HOD +/-	?	?

44.76	LRPPRC deficiency	Cavitating leukodystrophy, deep cerebrum	cortex: n	DWI: +/-	n-↓↓	cortex: n	DWI: +/-	n-↓↓	mb: +/-	DWI: +/-	n	?	MCD	Lactate
			wmse: +/-	T2: n-↑↑		wmse: n	T2: n-↑		p: n				PMG	
			wmd: +/-	Myelin: n		wmd: +/-	Myelin: n		m: +/-				Pachygyria	
			BG: +/-	Nec: -		D: +/-	Nec: -						CCD/HCC	
			Thal: n	Ca: -			Ca: -						Hippocampal malformation	
				CE:?			CE:?						Cerebellar hypoplasia	
44.77	TACO1 deficiency	Leigh-like	cortex: n	DWI: +/-	↓-↓↓	n	n	n	n	n	n	?	-	?
			wmse: +/-	T2: ↑-↑↑										
			wmd: +/-	Myelin: n										
			BG: ++	Nec: +										
			Thal: n	Ca: -										
				CE:?										
44.80	APOPT1 deficiency	Cavitating leukodystrophy, deep cerebrum	cortex: n	DWI: +	n-↓↓↓	n	n	n	mb: +/-	DWI: -	n	?	-	Lactate +/-
			wmse: +/-	T2: ↑-↑↑					p: +/-					
			wmd: ++	Myelin: n					m: +/-					
			BG: n	Nec: +										
			Thal: n	Ca: -										
				CE:?										
44.85	Mitochondrial ATP synthase F0 subunit 6 deficiency	Leigh-like	cortex: +/-	DWI: +/-	n-↓	cortex: +/-	DWI: -	n-↓	mb: +/-	DWI: -	n-↓	?	-	Lactate +/-
			wmse: +/-	T2: ↑-↑↑		wmse: +/-	T2: n-↑		p: +/-					NAA n-↓
			wmd: +/-	Myelin: n		wmd: +/-	Myelin: n		m: +/-					
			BG: +/-	Nec: +/-		D: n	Nec: -							
			Thal: +/-	Ca: -			Ca: -							
				CE:?			CE:?							
45.01, 45.03-45.07, 45.11-45.12	Mitochondrial DNA depletion syndromes	Occipital cortex, thalamus, inferior olives, deep cerebellar lesions	cortex: +/-	DWI: +/-	n-↓↓↓	cortex: +/-	DWI: -	n-↓	mb: +/-	DWI: -	n-↓	RST T2↑ +/-	Germinal cysts +/-	Lactate
		MELAS	wmse: +/-	T2: n-↑		wmse: +	T2: ↑		p: +/-					NAA n-↓
		Leigh-like	wmd: +/-	Myelin: n-↓		wmd: +	Myelin: n		m: +/-					Cho n-↓
			BG: +/-	Nec: +/-		D: +/-	Nec: -							
			Thal: +/-	Ca: -			Ca: -							
				CE:?			CE:?							
45.17	Mitochondrial RNA import protein deficiency	Striatum lesions	BG: +	T2: ↑	↓	n	n	n	n	n	n	?	-	?

(continued)

Table 8.1 (continued)

Chapter	Disease	Prevailing pattern(s)	Cerebrum			Cerebellum			Brainstem			Spinal cord	Malformations and other findings	MRS (ppm)
			Location	Texture	Volume	Location	Texture	Volume	Location	Texture	Volume			
45.24	Mitochondrial methionyl-tRNA formyltransferase deficiency	Leigh-like	cortex: n	DWI: +/- T2: ↑	n-↓	cortex: +/- wmisc: +/-	DWI: - T2: n-↑	n	mb: +/- p: +/-	DWI: - T2: n-↑	n	?	?	
		Multiple sclerosiformic	wmd: +/-	Myelin: n		wmd: n	Myelin: n		m: +/-	Myelin: n				
45.50-45.71	Mitochondrial tRNA deficiencies	Leukodystrophy	cortex: +/-	DWI: +/- T2: n-↑	n-↓	cortex: n wmisc: +/-	DWI: - T2: n-↑	n	mb: +/- p: +/-	DWI: - T2: n-↑	n	?	Optic atrophy +/- Aneurysms +/-	Lactate +/-
		MELAS	wmd: +/-	Myelin: n		wmd: +/-	Myelin: n		m: +/-	Myelin: n				
		Leigh-like	BG: +/- Thal: +/-	Nec: - Ca: +/- CE: ?		D: +/- Ca: - CE: ?	Nec: - Ca: - CE: ?			Nec: - Ca: - CE: ?				
45.72	Mitochondrial arginine-tRNA synthetase deficiency (AARS2)	Leukodystrophy, frontal and parietal dominant, relative sparing of frontoparietal junction	cortex: n	DWI: +/-	n-↓↓	n	n	n-↓↓	mb: +/-	DWI: -	n-↓	?	-	Cr ↑
		White matter tract involvement: CC, FP, POP, CST	wmisc: +/-	T2: ↑-↑↑						p: +/-	T2: n-↑			
45.75	Mitochondrial aspartyl-tRNA synthetase deficiency (DARS2)	Leukodystrophy, deep cerebrum (+/- PA gradient), CST, ASCT, ML, TGNF, cerebellar peduncles, DC, LCST	wmd: ++ BG: n Thal: n	Myelin: n-↓ Nec: + Ca: - CE: -					m: +/-	Myelin: n Nec: - Ca: - CE: -				Glycine (3.5)
		MRS: lactate	cortex: n	DWI: -	n-↓	cortex: n	DWI: -	n	mb: n	DWI: -	n		Diffuse T2↑ LCST and DC	Lactate
			wmisc: +/- wmd: ++	T2: ↑↑ Myelin: n		wmisc: n wmd: +	T2: ↑-↑↑ Myelin: n		p: + m: +	T2: ↑ Myelin: n				
			BG: +/- Thal: n	Nec: +/- Ca: - CE: ?		D: n	Nec: - Ca: - CE: ?			Nec: - Ca: - CE: ?				





Table 8.1 (continued)

Chapter	Disease	Prevailing pattern(s)	Cerebrum			Cerebellum			Brainstem			Spinal cord	Malformations and other findings	MRS (ppm)
46.9	MSTOI deficiency	Cerebellar atrophy +/- cortical hyperintensity	Location: cortex: n	Texture: DWI: -	Volume: n-↓	Location: cortex: +/-	Texture: DWI: -	Volume: ↓-↓↓	Location: n	Texture: n	Volume: n-↓	?	-	?
46.17-46.18	Mitochondrial processing peptidase alpha or beta deficiency	Cerebellar atrophy +/- cortical hyperintensity Leigh-like	Location: cortex: n wmisc: n wmd: +/- BG: n Thal: n	Texture: T2: n-↑ Myelin: n Nec: - Ca: - CE: ?	Volume: n-↓↓	Location: cortex: +/-	Texture: DWI: -	Volume: ↓↓-↓↓	Location: n	Texture: n	Volume: n-↓	?	-	Lactate +/-
46.24	HSP60 deficiency	Hypomyelinating leukodystrophy	Location: cortex: n wmisc: + wmd: + BG: n Thal: n	Texture: T2: ↑ Myelin: ↓ Nec: - Ca: - CE: ?	Volume: ↓-↓	Location: cortex: n	Texture: DWI: -	Volume: n	Location: mb: +	Texture: DWI: -	Volume: n-↓	?	-	?
47.1-47.4; 47.6-47.8	Primary coenzyme Q10 deficiency	Cerebellar atrophy Leigh-like MELAS	Location: cortex: +/- wmisc: +/- wmd: +/- BG: +/- Thal: +/-	Texture: T2: n-↑ Myelin: n Nec: - Ca: - CE: ?	Volume: n-↓	Location: cortex: +/- wmisc: + wmd: + D: n Ca: - CE: ?	Texture: T2: ↑ Myelin: ↓ Nec: - Ca: - CE: ?	Volume: ↓↓-↓↓	Location: mb: n p: n m: +/-	Texture: DWI: - T2: n-↑ Myelin: n Nec: - Ca: - CE: ?	Volume: n-↓	?	ACC +/-	?
48.1	Primary carnitine deficiency	Cerebral infarctions Arterial stenoses Cerebral white matter intramyelinic edema Hypoglycemic brain injury pattern	Location: cortex: +/- wmisc: + wmd: +/- BG: +/- Thal: n	Texture: DWI: + T2: ↑ Myelin: n Nec: - Ca: - CE: ?	Volume: n-↓	Location: cortex: n wmisc: +/- wmd: + D: n	Texture: DWI: + T2: ↑ Myelin: n Nec: -	Volume: n	Location: mb: +/- p: +/- m: +/-	Texture: DWI: +/- T2: n-↑ Myelin: n Nec: -	Volume: n	?	-	?
48.2	Carnitine palmitoyltransferase IA deficiency	MRS: lipids	Location: n	Texture: n Ca: - CE: -	Volume: n	Location: n	Texture: n Ca: - CE: -	Volume: n	Location: n	Texture: n Ca: - CE: -	Volume: n	?	-	Lipids ↑ NAA ↑ Glx ↑

48.4	Carnitine palmitoyltransferase 2 deficiency	MRS: lipids Brain malformations	DWI: -	n-↓	n	n	n	n	n	n-↓	n	n	n-↓	?	MCD: PMG, dysplasia, heterotopia +/- DWM +/- ACC +/- Vermian hypoplasia +/- Hemorrhages +/- Hydrocephalus +/- Arterial stenoses +/-	Lipids ↑
			cortex: +/- wmisc: +/- wmd: +/- BG: n Thal: n													
48.5	Carnitine-acylcarnitine translocase deficiency	Cerebral infarcts Arterial stenoses MRS: lipids	DWI: +	n-↓	n	n	n	n	n	n	n	n	n	?		Lipids ↑
			cortex: +/- wmisc: + wmd: +/- BG: +/- Thal: n													
48.9	Short-chain acyl-CoA dehydrogenase deficiency	Cavitating leukodystrophy, cerebrum anteroposterior gradient Leigh-like	DWI: +/-	n-↓↓↓	cortex: n	DWI: -	n	n	n	n	n	n	n	?	PMG +/-	?
			cortex: +/- wmisc: +/- wmd: +/- BG: +/- Thal: +/-													
48.10	Medium-chain acyl-CoA dehydrogenase deficiency	Leigh-like	DWI: +/-	n-↓	n	n	n	n	n	n	n	n	n	?	-	Glx n-↑ GABA (1.9) n-↑ Cr n-↑ MI n-↓
			cortex: n wmisc: n wmd: + BG: ++ Thal: +/-													
48.23	Fatty aldehyde dehydrogenase deficiency (Sjögren-Larsson syndrome)	Leukodystrophy MRS: lipids	DWI: -	n-↓	n	n	n	n	n	n	n	n	n	?	-	Lipids ↑ NAA n-↓ MI n-↑ Cr n-↑ Cho n-↑
			cortex: n wmisc: +/- wmd: ++ BG: n Thal: n													
50.3	Mitochondrial acetoacetyl-CoA thiolase deficiency (β-ketothiolase deficiency)	Leigh-like	DWI: +/-	n	n	n	n	n	n	n	n	n	n	?	-	?
			cortex: n wmisc: n wmd: n BG: ++ Thal: n													

(continued)







Table 8.1 (continued)

Chapter	Disease	Prevaling pattern(s)	Cerebrum	Cerebellum	Brainstem	Spinal cord	Malignancies and other findings	MRS (ppm)
56.5	Sterol 27-hydroxylase deficiency (cerebrotendinous xanthomatosis)	Dentate calcifications +/- necrosis Leukoencephalopathy, cerebrum and cerebellum	Location: cortex: n	Location: cortex: n	Location: mb: +/-	Lateral and DC T2↑ +/-	-	?
			wmse: +/-	wmse: +/-	p: +/-			
56.7	α-methylacyl-CoA racemase deficiency	Dentatorubrothalamic tract involvement without HOD	Location: cortex: +/-	Location: cortex: n	Location: mb: +/-			?
			wmse: +/-	wmse: n	p: +/-			
57.4	Porphobilinogen deaminase deficiency (acute intermittent porphyria)	Leukoencephalopathy, deep cerebrum (IC, CC, BG spared), thalami, and central pons	Location: cortex: +/-	Location: cortex: +/-	Location: n		Transient vasospasm +/-	?
			wmse: +/-	wmse: +/-	n			
59.1	EPG5 deficiency	ACC/HCC MCD Hypomyelination	Location: cortex: n	Location: cortex: n	Location: n		ACC/HCC +/-	?
			wmse: n	wmse: n	n		Absent TMI +/-	
59.2	WDR45 deficiency (BPAN)	NBAl (SN > GP iron deposition) T1↑ halo CP/SN	Location: cortex: n	Location: cortex: n	Location: mb: ++		Hippocampal dysgenesis +/-	?
			wmse: n	wmse: n	p: n			
			Location: wmd: n	Location: wmd: n	Location: m: n			
			Texture: DWI: -	Texture: DWI: -	Texture: Myelin: n			
			Texture: T2: n-↑	Texture: T2: ↓-n-↑	Texture: Myelin: n			
			Texture: Myelin: n	Texture: Myelin: n	Texture: Myelin: n			
			Texture: Nec: -	Texture: Nec: +/-	Texture: Nec: -			
			Texture: Ca: -	Texture: Ca: +/-	Texture: Ca: -			
			Texture: CE: -	Texture: CE: -	Texture: CE: -			
			Texture: DWI: +/-	Texture: DWI: -	Texture: DWI: -			
			Texture: T2: n-↑	Texture: T2: n-↑	Texture: T2: n-↑			
			Texture: Myelin: n	Texture: Myelin: n	Texture: Myelin: n			
			Texture: Nec: -	Texture: Nec: -	Texture: Nec: -			
			Texture: Ca: -	Texture: Ca: -	Texture: Ca: -			
			Texture: CE: -	Texture: CE: -	Texture: CE: -			
			Texture: DWI: -	Texture: DWI: +/-	Texture: n			
			Texture: T2: n-↑	Texture: T2: n-↑	Texture: n			
			Texture: Myelin: n	Texture: Myelin: n	Texture: Myelin: n			
			Texture: Nec: -	Texture: Nec: -	Texture: Nec: -			
			Texture: Ca: -	Texture: Ca: -	Texture: Ca: -			
			Texture: CE: -	Texture: CE: -	Texture: CE: -			
			Texture: DWI: -	Texture: DWI: -	Texture: n			
			Texture: T2: n-↑	Texture: T2: n-↑	Texture: n			
			Texture: Myelin: n	Texture: Myelin: n	Texture: Myelin: n			
			Texture: Nec: -	Texture: Nec: -	Texture: Nec: -			
			Texture: Ca: -	Texture: Ca: -	Texture: Ca: -			
			Texture: CE: +/-	Texture: CE: -	Texture: CE: -			
			Texture: DWI: -	Texture: DWI: -	Texture: n			
			Texture: T2: n-↑	Texture: T2: n-↑	Texture: n			
			Texture: Myelin: n-↓	Texture: Myelin: n-↓	Texture: n			
			Texture: Nec: -	Texture: Nec: -	Texture: n			
			Texture: Ca: -	Texture: Ca: -	Texture: n			
			Texture: CE: ?	Texture: CE: ?	Texture: n			
			Texture: DWI: -	Texture: DWI: -	Texture: n			
			Texture: T2: ↓-↓	Texture: T2: ↓-↓	Texture: n			
			Texture: Myelin: n-↓	Texture: Myelin: n-↓	Texture: m: n			
			Texture: Nec: -	Texture: Nec: -	Texture: Nec: -			
			Texture: Ca: +/-	Texture: Ca: +/-	Texture: Ca: -			
			Texture: CE: ?	Texture: CE: ?	Texture: CE: -			

59.22	Cohen syndrome	Thick CC, microcephaly	n	n	↓	n	n	↓	n	n	n	↓	n	n	↓	?	Thick CC	?
60.1–60.9; 60.13	Neuronal ceroid lipofuscinosis	Cerebral and cerebellar atrophy Thalamic hypointensity	cortex: n wmisc: n wmd: +/- BG: n Thal: n	DWI: - T2: n-↑ Myelin: n Nec: - Ca: - CE: -	n-↓↓↓	cortex: n wmisc: n wmd: n D: +/- Ca: - CE: -	DWI: - T2: n-↑ Myelin: n Nec: - Ca: - CE: -	↓-↓↓↓	n	n	n	n-↓	n	n	n	n	Vermis and BS hypoplasia PMG +/- Cerebellar hypoplasia +/- NAA ↓	NAA ↓
60.17–60.20	GM1 and/or GM2 gangliosidosis	Thalamic and dentate SA	cortex: n wmisc: n wmd: +/- BG: +/- Thal: +/-	DWI: - T2: ↑;(DGN) Myelin: n-↓ Nec: - Ca: +/- CE: -	↑-n-↓	cortex: n wmisc: n wmd: +/- D: n Ca: - CE: -	DWI: - T2: n-↑ Myelin: n Nec: - Ca: - CE: -	n-↓↓↓	mb: +/-	p: +/- m: n	DWI: - T2: n-↑ Myelin: n Nec: - Ca: - CE: -	n	n	n	n	n	-	MI n-↑ NAA n-↓ Cho n-↑
60.21	β-galactosylceramidase deficiency (Krabbe disease)	Leukodystrophy, deep cerebrum; PA gradient CST involvement, corona radiata to cerebral peduncles Tigroid white matter signal Cranial and/or spinal nerve enhancement Deep cerebral mineralization	cortex: n wmisc: +/- wmd: ++ BG: +/- Thal: +/-	DWI: +/- T2: ↑;(thl) Myelin: n-↓ Nec: - Ca: +/- CE: +/-	n-↓	cortex: n wmisc: n wmd: +/- D(thla): +/- Nec: - Ca: - CE: -	DWI: - T2: n-↑ Myelin: n Nec: - Ca: - CE: -	n	mb: +/- p: +/-	DWI: - T2: n-↑ Myelin: n Nec: - Ca: - CE: -	n	n	n	n	n	n	Cauda equina thickening/CE +/- Atrophy +/-	MI ↑ NAA n-↓ Cho ↓-n-↑ Glu n-↑ Lactate +/-
60.22	Arylsulfatase A deficiency (metachromatic leukodystrophy)	Leukodystrophy, deep cerebral white matter; PA gradient (pediatrics), AP gradient (adults) Tigroid white matter signal Cranial and/or spinal nerve enhancement Thalamic hypointensity	cortex: n wmisc: +/- wmd: ++ BG: n Thal: +/-	DWI: +/- T2: ↑;(thl) Myelin: n-↓ Nec: - Ca: - CE: +/-	n-↓	cortex: n wmisc: n wmd: +/- D: n Ca: - CE: -	DWI: - T2: n-↑ Myelin: n Nec: - Ca: - CE: -	n-↓	mb: +/- p: +/-	DWI: - T2: n-↑ Myelin: n Nec: - Ca: - CE: -	n-↓	n	n	n	n	n	Cauda equina thickening/enhancement +/- Optic nerve enlargement +/-	MI ↑ NAA n-↓ cho n-↑ Lactate +/- Glu n-↓

(continued)





		DWI: -	n-↓↓	cortex: n	DWI: -	↑-n-↓	mb: +/-	DWI: -	n	Dysostosis multiplex	Hypothalamic involvement +/-	Oligosaccharides and/or glycolipids (3,8) Fructose (1,2)	
61.6	α-fucosidase deficiency (fucosidosis)	Leukoencephalopathy, cerebrum	DWI: -	cortex: n	DWI: -	↑-n-↓	mb: +/-	DWI: -	n				
		DGN hypointensity	T2:↓(DGN); n-↑	wmsc: +/-	T2: n-↑		p: n	T2: n-↓					
		Thalamic and globus pallidus GP internal medullary lamina T2↑	TI(DGN): n-↑	wmd: +/-	Myelin: n-↓		m: n		Myelin: n-↓				
		MRS: oligosaccharides and fructose	Myelin: n-↓	BG: +/-	D: n	Nec: -			Nec: -				
		Dysostosis multiplex	Nec: -	Thal: +/-	Ca: -	Ca: -			Ca: -				
		CE: -		CE: -				CE: -					
61.7	Aspartylglucosaminidase deficiency	Leukoencephalopathy, cerebrum	DWI: -	cortex: n	DWI: -	n-↓↓	n	n	n-↓↓	?	-	?	
		DGN hypointensity	T2:↓(DGN); n-↑	wmsc: +									
		Pulvinar T2↓	TI(DGN): n-↑	wmd: +									
			BG: +/-	Myelin: ↓									
			Thal: +	Nec: -									
		Ca: -											
		CE: -											
61.8	Sialin deficiency; Infantile sialic acid storage disease (severe); Salla disease (milder)	Hypomyelination, cerebrum +/- cerebellum	DWI: -	cortex: n	DWI: -	n-↓	n	n	n	?	HCC +/-	NAA n-↑	
		Cerebellar atrophy	T2:↓(GP); n-↑	wmsc: +									MI n-↑
			TI(DGN): n-↑	wmd: +									Lactate +/-
			BG: +/-	Myelin: ↓									
			Thal: n	Nec: -									
		Ca: -											
		CE: -											
62.1-62.4, 62.9	Mucopolysaccharidoses I, II, IIIa, IIIb, VI	Enlarged PVS	DWI: -	cortex: n	DWI: -	n-↓	n	n	n	Dysostosis multiplex	Enlarged PVS	MI n-↑	
		Leukoencephalopathy, cerebrum	T2: n-↑	wmsc: +/-								Hydrocephalus +/-	NAA n-↓
		Hydrocephalus	Myelin: ↓	wmd: +								MCM +/-	Cho ↓ - n-↑
		Dysostosis multiplex	Nec: -	BG: +/-								Sellar malformation	Glu n-↓
			Ca: -	Thal: +/-								Chiari I +/-	
		CE: -											
64.6	X-linked adrenoleukodystrophy	Leukodystrophy, deep cerebrum, PA gradient >AP gradient	DWI: +/-	cortex: n	DWI: -	n-↓	mb: +/-	DWI: -	n	Atrophy +/-	-	Cho n-↑	
		Visual, auditory, and corticospinal tract involvement	T2: ↑ ↑ ↑	wmsc: +/-									NAA n-↓
		CE and/or restricted diffusion in areas of demyelination	Myelin: n-↓	wmd: +									MI n-↑
			Nec: +/-	BG: +/-									Lactate +/-
			Ca: +/-	Thal: n									
		CE: +/-											

(continued)

Table 8.1 (continued)

Chapter	Disease	Prevailing pattern(s)	Cerebrum			Cerebellum			Brainstem			Spinal cord	Malformations and other findings	MRS (ppm)
			Location	Texture	Volume	Location	Texture	Volume	Location	Texture	Volume			
64.13–64.25	Peroxisomal Biosynthesis disorders	Leukodystrophy, cerebrum (PA gradient or diffuse), brainstem, cerebellum	cortex: n	DWI: –	n-↓	cortex: n	DWI: –	n	mb: +/-	DWI: –	n	?	MDC; perisylvian polymicrogyria +/-	Lipids n-↑
		CST, ML, dentatorubrothalamic tract involvement	wmsc: +/-	T2: ↑-↑		wmsc: n	T2: ↑		p: +/-	T2: n-↑			Germinolytic cysts +/-	NAA ↓
			wmd: ++	Myelin: ↓		wmd: +	Myelin: n		m: +/-	Myelin: n				Cho ↑
			BG: n	Nec: –		D(hilus): +	Nec: –			Nec: –				
			Thal: +/-	Ca: –			Ca: –			Ca: –				
				CE: +/-			CE: –			CE: +/-				
64.14	Peroxin 1 deficiency (Zellweger Syndrome)	Abnormal myelination	cortex: n	DWI: n	n-↓	cortex: n	DWI: –	n-↓	n	n	n-↓	?	Germinolytic cysts +/-	Lipids n-↑
		MCD; polymicrogyria, perisylvian	wmsc: +	T2: ↑		wmsc: n	T2: n-↑						MDC; perisylvian polymicrogyria or pachygyria +/-	NAA ↓
		Germinolytic cysts	wmd: +	T1(BG): n-↑		wmd: +/-	Myelin: n						HCC +/-	Cho ↑
			BG: +/-	Myelin: ↓		D: n	Nec: –							Lactate +/-
			Thal: n	Nec: –			Ca: –							
				Ca: –			CE: –							
				CE: –										
66.29–66.37, 66.40	Alpha dystroglycanopathies (WWS, MEB, Fukuyama muscular dystrophy, etc.)	Variable diffuse brain malformation/hypoplasia	cortex: +	DWI: n	↓-↓	cortex: +	DWI: –	↓-↓	mb: +/-	DWI: –	↓-↓	?	MCD; cobblestone complex, PMG, pachygyria, dysplasia	NAA n-↓
		Cobblestone complex	wmsc: +/-	T2: ↑		wmsc: +	T2: ↑		p: +/-	T2: n-↑			Cerebellar hypoplasia/dysplasia +/- cysts	Cho n-↑
		Brainstem and cerebellum hypoplasia/dysplasia	wmd: +	Myelin: ↓		wmd: +	Myelin: n-↓		m: +/-	Myelin: n-↓			Brainstem hypoplasia/dysplasia; Z-shape +/- AP patterning defects +/-, pontine cleft +/-	
		Z-shaped brainstem, pontine cleft, and/or AP patterning defects	BG: n	Nec: –		D: n	Nec: –			Nec: –			CCD +/-	
		Cerebellar cysts	Thal: n	Ca: –			Ca: –			Ca: –			Hydrocephalus +/-	
		Hypomyelination and leukoencephalopathy		CE: –			CE: –			CE: +/-			Oculomalignations +/-	



## References

- Anderson PJ, Leuzzi V. White matter pathology in phenylketonuria. *Mol Genet Metab*. 2010;99(Suppl 1):S3–9.
- Anghileri E, Bertolino N, Salsano E, Antelmi L, Carpinelli P, Castellotti B, Zucca I, Gellera C, Bisogno R, Caccia C, Cuccarini V. In-vivo brain H1-MR-Spectroscopy identification and quantification of 2-hydroxyglutarate in L-2-Hydroxyglutaric aciduria. *Brain Res*. 2016;1648(Pt A):506–11.
- Autti T, Joensuu R, Aberg L. Decreased T2 signal in the thalami may be a sign of lysosomal storage disease. *Neuroradiology*. 2007;49(7):571–8.
- Barkovich JA, Patay Z. Metabolic, toxic, and autoimmune/inflammatory brain disorders. In: Barkovich AJ, Raybaud C, editors. *Pediatric neuroimaging*. 6th ed. Philadelphia: Lippincott Williams & Wilkins; 2019.
- Bhat M, Prasad C, Bindu PS, Aziz Z, Christopher R, Saini J. Unusual imaging findings in brain and spinal cord in two siblings with maple syrup urine disease. *J Neuroimaging*. 2013;23(4):540–2.
- Bireley WR, Van Hove JL, Gallagher RC, Fenton LZ. Urea cycle disorders: brain MRI and neurological outcome. *Pediatr Radiol*. 2012;42(4):455–62.
- Bluml S, Panigrahy A. MR spectroscopy of pediatric brain disorders. New York: Springer Publishing; 2013.
- Brismar J, Brismar G, Gascon G, Ozand P. Canavan disease: CT and MR imaging of the brain. *AJNR Am J Neuroradiol*. 1990;11(4):805–10.
- Cohn RD, Eklund E, Bergner AL, Casella JF, Woods SL, et al. Intracranial hemorrhage as the initial manifestation of a congenital disorder of glycosylation. *Pediatrics*. 2006;118(2):e514–21.
- Dallabona C, Diodato D, Kevelam SH, Haack TB, Wong LJ, et al. Novel (ovario) leukodystrophy related to AARS2 mutations. *Neurology*. 2014;82(23):2063–71.
- Feraco P, Mirabelli-Badenier M, Severino M, Alpigiani MG, Di Rocco M, Biancheri R, Rossi A. The shrunken, bright cerebellum: a characteristic MRI finding in congenital disorders of glycosylation type Ia. *AJNR Am J Neuroradiol*. 2012;33(11):2062–7.
- Fourati H, Ellouze E, Ahmadi M, Chaari D, Kamoun F, Hsairi I, Triki C, Mnif Z. MRI features in 17 patients with l2 hydroxyglutaric aciduria. *Eur J Radiol Open*. 2016;3:245–50.
- Gagliardi D, Mauri E, Magri F, Velardo D, Meneri M, et al. Can intestinal pseudo-obstruction drive recurrent stroke-like episodes in late-onset MELAS syndrome? A case report and review of the literature. *Front Neurol*. 2019;10:38.
- Gropman AL. Patterns of brain injury in inborn errors of metabolism. *Semin Pediatr Neurol*. 2012;19(4):203–10.
- Gropman AL, Seltzer RR, Yudkoff M, Sawyer A, VanMeter J, Fricke ST. 1H MRS allows brain phenotype differentiation in sisters with late onset ornithine transcarbamylase deficiency (OTCD) and discordant clinical presentations. *Mol Genet Metab*. 2008a;94(1):52–60.
- Gropman AL, Fricke ST, Seltzer RR, Hailu A, Adeyemo A, Sawyer A, van Meter J, Gaillard WD, McCarter R, Tuchman M, Batschaw M, Urea Cycle Disorders Consortium. 1H MRS identifies symptomatic and asymptomatic subjects with partial ornithine transcarbamylase deficiency. *Mol Genet Metab*. 2008b;95(1–2):21–30.
- Gungor S, Akinci A, Firat AK, Tabel Y, Alkan A. Neuroimaging findings in hyperargininemia. *J Neuroimaging*. 2008;18(4):457–62.
- Gunz AC, Choong K, Potter M, Miller E. Magnetic resonance imaging findings and neurodevelopmental outcomes in neonates with urea-cycle defects. *Int Med Case Rep J*. 2013;6:41–8.
- Ha JS, Kim TK, Eun BL, Lee HS, Lee KY, Seol HY, Cha SH. Maple syrup urine disease encephalopathy: a follow-up study in the acute stage using diffusion-weighted MRI. *Pediatr Radiol*. 2004;34(2):163–6.
- Harting I, Boy N, Heringer J, Seitz A, Bendszus M, Pouwels PJ, Kolker S. (1)H-MRS in glutaric aciduria type 1: impact of biochemical phenotype and age on the cerebral accumulation of neurotoxic metabolites. *J Inher Metab Dis*. 2015;38(5):829–38.
- Hayflick SJ, Kurian MA, Hogarth P. Neurodegeneration with brain iron accumulation. *Handb Clin Neurol*. 2018;147:293–305.
- Heindel W, Kugel H, Roth B. Noninvasive detection of increased glycine content by proton MR spectroscopy in the brains of two infants with nonketotic hyperglycinemia. *AJNR Am J Neuroradiol*. 1993;14(3):629–35.
- Helman G, Pacheco-Colon I, Gropman AL. The urea cycle disorders. *Semin Neurol*. 2014;34(3):341–9.
- Herini E, Tsuneishi S, Takada S, Sunarini, Nakamura H. Clinical features of infants with subependymal germinolysis and choroid plexus cysts. *Pediatr Int*. 2003;45(6):692–6.
- Holzbach U, Hanefeld F, Helms G, Hanicke W, Frahm J. Localized proton magnetic resonance spectroscopy of cerebral abnormalities in children with carbohydrate-deficient glycoprotein syndrome. *Acta Paediatr*. 1995;84(7):781–6.
- Ishikawa A, Okayasu T, Miyasak K, Fukushima N, Takase A, Wagatsuma Y. A mild variant case of maple syrup urine disease. *No To Hattatsu*. 1991;23(1):71–4.
- Ito H, Mori K, Sakata M, Naito E, Harada M, Kagami S. Transient left temporal lobe lesion in Menkes disease may influence the generation of tonic spasms. *Brain Dev*. 2011;33(4):345–8.
- Jan W, Zimmerman RA, Wang ZJ, Berry GT, Kaplan PB, Kaye EM. MR diffusion imaging and MR spectroscopy of maple syrup urine disease during acute metabolic decompensation. *Neuroradiology*. 2003;45(6):393–9.
- Kassem H, Wafaie A, Abdelfattah S, Farid T. Leukoencephalopathy with brainstem and spinal cord involvement and lactate elevations (LBSL): assessment of the involved white matter tracts by MRI. *Eur J Radiol*. 2014;83(1):191–6.
- Kono K, Okano Y, Nakayama K, Hase Y, Minamikawa S, Ozawa N, Yokote H, Inoue Y. Diffusion-weighted MR imaging in patients with phenylketonuria: relationship between serum phenylalanine levels and ADC values in cerebral white matter. *Radiology*. 2005;236(2):630–6.
- La Piana R, Uggetti C, Roncarolo F, Vanderver A, Olivieri I, et al. Neuroimaging patterns and novel imaging findings in Aicardi-Goutieres syndrome. *Neurology*. 2016;86(1):28–35.
- Lange T, Dydak U, Roberts TPL, Rowley HA, Bjeljac M, Boesinger P. Pitfalls in lactate measurements at 3T. *AJNR Am J Neuroradiol*. 2006;27:895–901.
- Li PH, Ma JS, Chi CS, Mak SC. Intermittent form of maple syrup urine disease: report of one case. *Zhonghua Min Guo Xiao Er Ke Yi Xue Hui Za Zhi*. 1997;38(6):468–71.
- Loes DJ, Hite S, Moser H, Stillman AE, Shapiro E, Lockman L, Latchaw RE, Krivit W. *AJNR Am J Neuroradiol*. 1994;15(9):1761–6.
- Manara R, D'Agata L, Rocco MC, Cusmaj R, Freri E, et al. Menkes Working Group in the Italian Neuroimaging Network for Rare Diseases. Neuroimaging changes in Menkes disease, part 1. *AJNR Am J Neuroradiol*. 2017a;38(10):1850–7.
- Manara R, D'Agata L, Rocco MC, Cusmaj R, Freri E, et al. Menkes Working Group in the Italian Neuroimaging Network for Rare Diseases. Neuroimaging changes in Menkes disease, part 2. *AJNR Am J Neuroradiol*. 2017b;38(10):1858–65.
- McAdams HP, Geyer CA, Done SL, Deigh D, Mitchell M, Ghaed VN. CT and MR imaging of Canavan disease. *AJNR Am J Neuroradiol*. 1990;11(2):397–9.
- Muller K, Kahn T, Wendel U. Is demyelination a feature of maple syrup urine disease. *Pediatr Neurol*. 1993;9(5):375–82.
- Munakata M, Sakamoto O, Kitamura T, Ishitobi M, Yokoyama H, et al. The effects of copper-histidine therapy on brain metabolism in a patient with Menkes disease: a proton magnetic resonance spectroscopic study. *Brain Dev*. 2005;27(4):297–300.

- Myers KA, Reeves M, Wei XC, Khan A. Cerebral edema in maple syrup urine disease despite newborn screening diagnosis and early initiation of treatment. *JIMD Rep.* 2012;3:103–6.
- Nguyen HV, Ishak GE. Canavan disease—unusual imaging features in a child with mild clinical presentation. *Pediatr Radiol.* 2015;45(3):457–60.
- Pacheco-Colon I, Fricke S, VanMeter J, Gropman AL. Advances in urea cycle neuroimaging: proceedings from the 4<sup>th</sup> International Symposium on urea cycle disorders, Barcelona, Spain. *Mol Genet Metab.* 2013;113(1–2):118–26.
- Raymond GV, Moser AB, Fatemi A. X-linked adrenoleukodystrophy. In: Adam MP, Ardinger HH, Pagon RA, Wallace SE, Bean LJH, Stephens K, Amemiya A, editors. *GeneReviews®* [Internet]. Seattle: University of Washington, Seattle; 1993–2019; 1999. [Updated 2018 Feb 15].
- Robertson NJ, Staffer P, Battini R, Cheong J, Tosetti M, Bianchi MC, Cox IJ, Cowan FM, Cioni G. Brain lactic alkalosis in Aicardi-Goutieres syndrome. *Neuropediatrics.* 2004;35(1):20–6.
- Sakai M, Inoue Y, Oba H, Ishiguro A, Sekiguchi K, Tsukune Y, Mitomo M, Nakamura H. Age dependence of diffusion-weighted magnetic resonance imaging findings in maple syrup urine disease encephalopathy. *J Comput Assist Tomogr.* 2005;29(4):524–7.
- Salvan AM, Chabrol B, Lamoureux S, Confort-Gouny S, Cozzone PJ, Vion-Dury J. In vivo brain proton MR spectroscopy in a case of molybdenum cofactor deficiency. *Pediatr Radiol.* 1999;29(11):846–8.
- Samanta D, Ramakrishnaiah R. Recurrent encephalopathy with spinal cord involvement: an atypical manifestation of Aicardi-Goutieres syndrome. *Ann Indian Acad Neurol.* 2019;22(1):111–5.
- Schuijter G, Kurlmann G, Bick U, Stephani U. Molybdenum-cofactor deficiency: CT and MR findings. *Neuropediatrics.* 1995;26(1):51–4.
- Sener RN. Diffusion magnetic resonance imaging in intermediate form of maple syrup urine disease. *J Neuroimaging.* 2002;12(4):368–70.
- Sener RN. Phenylketonuria: diffusion magnetic resonance imaging and proton magnetic resonance spectroscopy. *J Comput Assist Tomogr.* 2003;27(4):541–3.
- Sener RN. Diffusion magnetic resonance imaging patterns in metabolic and toxic brain disorders. *Acta Radiol.* 2004;45(5):561–70.
- Sijens PE, Reijngoud DJ, Soorani-Lunsing RJ, Oudkerk M, van Spronsen FJ. Cerebral 1H MR spectroscopy showing elevation of brain guanidinoacetate in argininosuccinate lyase deficiency. *Mol Genet Metab.* 2006;88(1):100–2.
- Steenweg ME, Ghezzi D, Haack T, Abbink TE, Martinelli D, et al. Leukoencephalopathy with thalamus and brainstem involvement and high lactate ‘LTBL’ caused by EARS2 mutations. *Brain.* 2012;135(Pt 5):1387–94.
- Stefanits H, Konstantopoulou V, Kuess M, Milenkovic I, Matula C. Initial diagnosis of the congenital disorder of glycosylation PMM2-CDG (CDG1a) in a 4-year-old girl after neurosurgical intervention for cerebral hemorrhage. *J Neurosurg Pediatr.* 2014;14(5):546–9.
- Stence NV, Coughlin CR, Fenton LZ, Thomas JA. Distinctive pattern of restricted diffusion in a neonate with molybdenum cofactor deficiency. *Pediatr Radiol.* 2013;43(7):882–5.
- Stence NV, Fenton LZ, Levek C, Tong S, Coughlin CR 2nd, Hennermann JB, Wortmann SB, Van Hove JLK. Brain imaging in classic nonketotic hyperglycinemia: quantitative analysis and relation to phenotype. *J Inher Metab Dis.* 2019;42(3):438–50.
- Takanashi J, Barkovich AJ, Cheng SF, Weisiger K, Zlatunich CO, Mudge C, Rosenthal P, Tuchman M, Packman S. Brain MR imaging in neonatal hyperammonemic encephalopathy resulting from proximal urea cycle disorders. *AJNR Am J Neuroradiol.* 2003;24(6):1184–7.
- Takeuchi M, Harada M, Hisaoka S, Nishitani H, Mori K, Sakama M. Magnetic resonance imaging and proton MR spectroscopy of the brain in a patient with carbohydrate-deficient glycoprotein syndrome type I. *J Magn Reson Imaging.* 2003;17(6):722–5.
- Terek D, Koroglu O, Yazal M, Gokben S, Calli C, Coker M, Kultursay N. Diagnostic tools of early brain disturbances in an asymptomatic neonate with maple syrup urine disease. *Neuropediatrics.* 2013;44(4):208–12.
- Thorburn DR, Rahman J, Rahman S. In: Adam MP, Ardinger HH, Pagon RA, Wallace SE, Bean LJH, Stephens K, Amemiya A, editors. *Mitochondrial DNA-associated Leigh syndrome and NARP.* *GeneReviews®* [Internet]. Seattle: University of Washington, Seattle; 1993–2019; 2003. [Updated 2017 Sept 28].
- Toft PB, Geiss-Holtorff R, Rolland MO, Pryds O, Muller-Forell W, et al. Magnetic resonance imaging in juvenile Canavan disease. *Eur J Pediatr.* 1993;152(9):750–3.
- van der Knaap MS, Bugiani M. Leukodystrophies: a proposed classification system based on pathologic changes and pathogenetic mechanisms. *Acta Neuropathol.* 2017;134(3):351–82.
- Vanderver A, Prust M, Kadom N, Demarest S, Crow YJ, et al. Early-onset Aicardi-Goutieres syndrome: magnetic resonance imaging (MRI) patterns recognition. *J Child Neurol.* 2015;30(10):1343–8.
- Wei SH, Weng WC, Lee NC, Hwu WL, Lee WT. Unusual spinal cord lesions in late-onset non-ketotic hyperglycinemia. *J Child Neurol.* 2011;26(7):900–3.
- Whitehead MT, Gropman AL. Other metabolic syndromes. In: Lewis J, Keshari K, editors. *Imaging and metabolism.* Cham: Springer; 2018.
- Whitehead MT, Fricke ST, Gropman AL. Structural brain defects. *Clin Perinatol.* 2015;42(2):337–361, ix.
- Whitehead MT, Lee B, Gropman A. Lesional perfusion abnormalities in Leigh disease demonstrated by arterial spin labeling correlate with disease activity. *Pediatr Radiol.* 2016;46(9):1309–16.
- Whitehead MT, Wien M, Lee B, Bass N, Gropman A. Black toenail sign in MELAS syndrome. *Pediatr Neurol.* 2017a;75:61–5.
- Whitehead MT, Wien M, Lee B, Bass N, Gropman A. Cortical venous disease severity in MELAS syndrome correlates with brain lesion development. *Neuroradiology.* 2017b;59(8):813–8.
- Zafeiriou DI, Batziou SP. Brain and spinal MR imaging findings in mucopolysaccharidoses: a review. *AJNR Am J Neuroradiol.* 2013;34(1):5–13.